

## ***Ehrlichia* SLiM ligand mimetic activates Notch signaling in human monocytes**

LaNisha L. Patterson<sup>1</sup>, Thangam Sudha Velayutham<sup>1</sup>, Caitlan D. Byerly<sup>1</sup>, Duc Cuong Bui<sup>1</sup>, Jignesh Patel<sup>1</sup> Veljko Veljkovic<sup>6</sup>, Slobodan Paessler<sup>1</sup>, and Jere W. McBride<sup>1-5</sup>

<sup>1</sup>Departments of Pathology and <sup>2</sup>Microbiology and Immunology,

<sup>3</sup>Center for Biodefense and Emerging Infectious Diseases,

<sup>4</sup>Sealy Institute for Vaccine Sciences,

<sup>5</sup>Institute for Human Infections and Immunity,

University of Texas Medical Branch, Galveston, TX 77555

<sup>6</sup>Biomed Protection, LLC, Galveston, TX

Correspondence:

Jere W. McBride, Ph.D.

Department of Pathology

University of Texas Medical Branch

Galveston, TX 77555-0609

Tel: (409) 747-2498

Email: jemcbrid@utmb.edu

1 **Abstract**

2 *Ehrlichia chaffeensis* evades innate host defenses by reprogramming the mononuclear  
3 phagocyte through mechanisms that involve exploitation of multiple evolutionarily conserved  
4 cellular signaling pathways including Notch. This immune evasion strategy is directed in part by  
5 tandem repeat protein (TRP) effectors. Specifically, the TRP120 effector activates and regulates  
6 Notch signaling through interactions with the Notch receptor and the negative regulator, F-Box  
7 and WD repeat domain-containing 7 (FBW7). However, the specific molecular interactions and  
8 motifs required for *E. chaffeensis* TRP120-Notch receptor interaction and activation have not  
9 been defined. To investigate the molecular basis of TRP120 Notch activation, we compared  
10 TRP120 with endogenous canonical/non-canonical Notch ligands and identified a short region  
11 of sequence homology within the tandem repeat (TR) domain. TRP120 was predicted to share  
12 biological function with Notch ligands, and a function-associated sequence in the TR domain  
13 was identified. To investigate TRP120-Notch receptor interactions, colocalization between  
14 TRP120 and endogenous Notch-1 was observed. Moreover, direct interactions between full  
15 length TRP120, the TRP120 TR domain containing the putative Notch ligand sequence, and the  
16 Notch receptor LBR were demonstrated. To molecularly define the TRP120 Notch activation  
17 motif, peptide mapping was used to identify an 11-amino acid short linear motif (SLiM) located  
18 within the TRP120 TR that activated Notch signaling and downstream gene expression. Peptide  
19 mutants of the Notch SLiM or anti-Notch SLiM antibody reduced or eliminated Notch activation  
20 and NICD nuclear translocation. This investigation reveals a novel molecularly defined pathogen  
21 encoded Notch SLiM mimetic that activates Notch signaling consistent with endogenous  
22 ligands.

23

24

- 25 **Keywords:** *Ehrlichia*; tandem repeat protein; effector; Notch signaling; ligand; short linear motif;  
26 molecular mimicry

## 27 **Importance**

28 *E. chaffeensis* infects and replicates in mononuclear phagocytes, but how it evades innate  
29 immune defenses of this indispensable primary innate immune cell is not well understood. This  
30 investigation reveals the molecular details of a ligand mimicry cellular reprogramming strategy  
31 that involves a short linear motif (SLiM) which enables *E. chaffeensis* to exploit host cell  
32 signaling to establish and maintain infection. *E. chaffeensis* TRP120 is a moonlighting effector  
33 that has been associated with cellular activation and other functions including ubiquitin ligase  
34 activity. Herein, we identify and demonstrate that a SLiM present within each tandem repeat of  
35 TRP120 activates Notch signaling. Notch is an evolutionarily conserved signaling pathway  
36 responsible for many cell functions including cell fate, development, and innate immunity. The  
37 proposed study is significant because it reveals the first molecularly defined pathogen encoded  
38 SLiM that appears to have evolved *de novo* to mimic endogenous Notch ligands. Understanding  
39 Notch activation during *E. chaffeensis* infection provides a model in which to study pathogen  
40 exploitation of signaling pathways and will be useful in developing molecularly-targeted  
41 countermeasures for inhibiting infection by a multitude of disease-causing pathogens that  
42 exploit cell signaling through molecular mimicry.

43

44 **Author Summary**

45 *E. chaffeensis* is a small, obligately intracellular, Gram-negative bacterium that has evolved  
46 cellular reprogramming strategies to subvert innate defenses of the mononuclear phagocyte.  
47 Ehrlichial TRP effectors interface with the host cell and are involved in pathogen-host interplay  
48 that facilitates exploitation and manipulation of cellular signaling pathways; however, the  
49 molecular interactions and functional outcomes are not well understood. This study provides  
50 molecular insight into a eukaryotic mimicry strategy whereby secreted effectors of obligately  
51 intracellular pathogens activate the evolutionarily conserved Notch signaling pathway through a  
52 short linear motif ligand mimetic to promote intracellular infection and survival.

## 53 **Introduction**

54 *Ehrlichia chaffeensis* is a small, obligately intracellular, Gram-negative tick transmitted  
55 bacterium (1) that exhibits tropism for mononuclear phagocytes. *E. chaffeensis* establishes  
56 infection through a multitude of cellular reprogramming strategies that involve effector-host  
57 interactions resulting the in activation and manipulation of cell signaling pathways to suppress  
58 and evade innate immune mechanisms (2-8). The mechanisms whereby *E. chaffeensis* evades  
59 host defenses of the macrophage involves exploitation of Wnt and Notch signaling by the  
60 tandem repeat protein (TRP) effector, TRP120 (2-6).

61 *E. chaffeensis* TRP120 effector has well-documented moonlighting functions that include  
62 roles as a nucleomodulin (9, 10), a HECT E3 ubiquitin ligase (2, 7, 11), and as a ligand mimic  
63 (3, 5, 6, 12). Previously, we found that TRP120 is involved in a diverse array of host cell  
64 interactions including components of signaling and transcriptional regulation associated with  
65 Wnt and Notch signaling pathways (8). We have recently shown that TRP120 ubiquitinates the  
66 Notch negative regulator FBW7 resulting in increased NICD levels, as well as other FBW7  
67 regulated oncoproteins during infection (2). In addition, we have also demonstrated that *E.*  
68 *chaffeensis* Notch activation results in downregulation of toll-like receptor 2 and 4 expression,  
69 likely as an immune evasion mechanism (6). Although we have demonstrated TRP120 activates  
70 Notch signaling, the molecular details involved in activation have yet to be defined.

71 The Notch signaling pathway is evolutionarily conserved and is known to play a critical  
72 role in cell proliferation, differentiation, and apoptosis in all metazoan organisms (13-16). Notch  
73 activation plays significant roles in various other cellular outcomes, including MHC Class II  
74 expansion (17), B- and T- cell development (18), and innate immune mechanisms such as  
75 autophagy (19) and apoptosis (20, 21). Canonical Notch activation is driven by direct cell-  
76 membrane bound receptor-ligand interactions with four Notch receptors (Notch1-4) and  
77 canonical Notch ligands, Delta-like (DLL 1,3,4) and Jagged (Jagged/Serrate-1 and 2). Notch

78 receptor-ligand interactions occur at the Notch extracellular domain (NECD), specifically at  
79 epidermal growth factor-like repeats (EGFs) 11-13, the known ligand binding domain (LBD).  
80 Module at the N-terminus of Notch ligands (MNNL) and Delta/Serrate/LAG-2 (DSL) domains in  
81 canonical Notch ligands interact with the Notch LBD. Although there is evidence demonstrating  
82 the requirement of both N-terminal MNNL and DSL Notch ligand domains for Notch receptor  
83 binding, there is little information known about ligand regions/motifs that are necessary for  
84 Notch activation (22, 23). During canonical Notch activation, ligands expressed on neighboring  
85 cells bind the Notch receptor and create a mechanical force at the negative regulatory region  
86 (NRR) which triggers several sequential proteolytic cleavages, releasing the Notch intracellular  
87 domain (NICD). NICD subsequently translocates to the nucleus and binds to other  
88 transcriptional coactivators, including RBPjK and MAML, to activate Notch gene transcription.  
89 Notably, secreted non-canonical Notch ligands have also been shown to activate Notch  
90 signaling; however, the molecular details of non-canonical Notch ligand-receptor interactions  
91 are not well defined.

92         There are three major classes of protein interaction modules which include globular  
93 domains, IDD, and short linear motifs (SLiMs), all of which have distinct biophysical attributes  
94 (24-26). IDDs are 20-50 amino acids in length, are known to be disordered in nature, are  
95 located within globular domains or intrinsically disordered protein regions and have transient  
96 interactions in the nanomolar range. In comparison, SLiMs are ~3-12 amino acids in length, are  
97 known to be disordered in nature, located within globular domains or IDDs, and have low  
98 micromolar affinity ranges with transient interactions. SLiMs have been shown to evolve *de*  
99 *novo* for promiscuous binding to various partners (26, 27). Ehrlichial TRPs interact with a  
100 diverse array of host proteins through several well-known protein-protein interaction  
101 mechanisms including post-translational modifications (PTMs), and various protein interaction  
102 modules located in intrinsically disordered domains (IDDs) (7, 9, 26, 28).

103           Microorganisms have developed mechanisms to survive in the host cell which involve  
104 hijacking host cell processes. Molecular mimicry has been well-established as an evolutionary  
105 survival strategy utilized by pathogens to disrupt or co-opt host function for infection and survival  
106 [26-29]. Studies have determined this occurs through pathogen effectors that mimic eukaryotic  
107 host proteins, allowing for pathogens to hijack and manipulate host cellular pathways and  
108 functions. SLiMs have been identified as interaction modules whereby eukaryotes and  
109 pathogens direct cellular processes through protein-protein interactions (29, 30). Recently, we  
110 have demonstrated TRP120 is a Wnt ligand mimetic that interacts with host Wnt receptors to  
111 activate Wnt signaling (3).

112           In this study, we reveal an *E. chaffeensis* Notch SLiM ligand mimetic whereby TRP120  
113 activates Notch signaling for infection and intracellular survival. Understanding the molecular  
114 mechanisms utilized by *E. chaffeensis* to subvert innate host defense for infection and survival  
115 is essential for understanding intracellular pathogen infection strategies and provides a model to  
116 investigate molecular host-pathogen interactions involved in repurposing host signaling  
117 pathways for infection.

## 118 **Results**

### 119 ***E. chaffeensis* TRP120 shares sequence homology and predicted Notch ligand function.**

120 We have previously shown TRP120 interacts with Notch activating metalloprotease, ADAM17  
121 and Notch antagonist FBW7 using yeast-two hybrid analysis (Y2H) (8). We have also shown  
122 that TRP120 binds to the promoter region of *notch1* using chromatin immunoprecipitation  
123 sequencing (ChIP-Seq), and that activation of Notch occurs during infection (6, 10). Notch  
124 activation occurs through direct interaction of Notch ligands with the Notch-1 receptor initiating  
125 two receptor proteolytic cleavages, resulting in NICD nuclear translocation and subsequent  
126 activation of Notch downstream targets. Since TRP120 has been shown to activate the Notch



127 signaling pathway, we examined TRP120 sequence homology and correlates of biological  
128 functionality with Notch ligands.

129 NCBI Protein Basic Local Alignment Search Tool (BLAST) was used to identify local  
130 similarity between TRP120 and canonical/non-canonical Notch ligand sequences. Sequence  
131 homology with a TRP120 tandem repeat (TR) IDD motif, TESHQKEDEIVSQPSSE (aa. 284-  
132 301), was shown to share sequence homology with several canonical Notch ligands, including  
133 Jagged-1, DLL1, DLL4, and non-canonical Notch ligand TSP2 (Fig. 1A). We then used  
134 informational spectrum method (ISM) to predict similar functional properties between TRP120  
135 and Notch ligands. ISM is a prediction method that uses the electron ion interaction potential of  
136 each amino acid within the primary sequence of proteins to translate the primary sequences into  
137 numerical sequences. Translated sequences are then converted into a spectrum using Fourier  
138 transform. Cross spectral analysis of the translated sequences is then performed to obtain  
139 characteristic frequency peaks that demonstrate if proteins share a similar biological function.  
140 TRP120 was predicted to share a similar biological function with canonical Notch ligands, DLL1,  
141 3 and 4, and non-canonical Notch ligand F3 contactin-1, a known adhesion molecule (Figs. S1  
142 A-D). To identify the sequence responsible for the identified frequency peaks, reverse Fourier  
143 transform of ISM was performed (Fig. 1B). A 35-mer TRP120-TR IDD motif,  
144 IVSQPSSEPFVAESEVSKVEQEETNPEVLIKDLQD (aa. 214-248 and 294-328), was associated  
145 with characteristic frequency peaks (Figs. 1B and 1C). Collectively, these results indicate that  
146 the TRP120 sequence and fundamental biophysical properties of the amino acids are consistent  
147 with Notch ligands.

#### 148 ***E. chaffeensis* TRP120 directly interacts with the Notch-1 ligand binding region (LBR).**

149 Canonical activation of the Notch pathway is known to occur through canonical Notch ligands  
150 binding to Notch receptor LBD (EGFs 11-13 in the extracellular domain). To investigate if  
151 TRP120 interacts with the Notch-1 receptor LBR (EGFs 1-15), we ectopically expressed GFP-

152 tagged full length TRP120 (TRP120-FL-GFP) in HeLa cells and probed for endogenous Notch-1  
153 to determine colocalization. Pearson's correlation coefficient (PC) and Mander's coefficient (MC)  
154 (correlation range +1 to -1; 0 represents absence of correlation), was used to quantify the  
155 degree of colocalization between TRP120-FL-GFP and Notch-1. Ectopically expressed  
156 TRP120-FL-GFP was found to strongly colocalize (PC = 0.897 and MC = 0.953) with  
157 endogenous Notch-1 (Fig. 2A). Colocalization of TRP120 and Notch-1 demonstrates that these  
158 two proteins are in the same spatial location; however, it does not demonstrate direct protein-  
159 protein interaction. To confirm a direct interaction, we utilized pull-down assays of TRP120-FL  
160 and Notch-1 LBR. A His-tagged rTRP120-FL (rTRP120-FL-His) construct was incubated with a  
161 Fc-tagged recombinant Notch-1 LBR, and a direct protein-protein interaction was demonstrated  
162 (Figs. 2B and S2A-B). Thioredoxin (TRX), used as a fusion tag in the pBAD expression vector  
163 containing TRP120 constructs and as a recombinant control, did not interact (Fig. 2B). Based on  
164 sequence homology and ISM data, a short region of sequence homology within the tandem  
165 repeat (TR) domain was identified that could be involved in the TRP120 and Notch-1 LBR. To  
166 determine if the TRP120-TR was responsible for the previous TRP120 and Notch-1 LBR  
167 interaction, we performed a pull-down assay with TRP120-TR and Notch-1 LBR. rTRP120-TR  
168 was pulled down with anti-Notch-1 LBR antibody demonstrating a direct interaction with the TR  
169 domain (Fig. 2C).

170 To further confirm direct interaction of TRP120-FL or TRP120-TR and Notch-1 LBR,  
171 surface plasmon resonance was performed. An interaction between both rTRP120-FL (Fig. 2D)  
172 and rTRP120-TR (Fig. 2E) with Notch-1 LBR was detected in a concentration dependent  
173 manner. Fitting the concentration response plots for TRP120-FL and TRP120-TR yielded a  $K_D$   
174 (equilibrium dissociation constant) of  $100 \pm 3.5$  nM and  $120 \pm 2.0$  nM, respectively (Figs. 2D-E).  
175 No interaction was detected between TRX and Notch-1 LBR (Fig. 2F). Additionally, treatment of  
176 THP-1 cells with TRP120-coated sulfate, yellow-green microspheres demonstrated

177 colocalization of TRP120 and Notch-1 (Figs. 2G-H). In comparison, TRX-coated fluorescent  
178 microsphere did not colocalize with the Notch-1 receptor (Figs. 2G-H). Together, these binding  
179 data reveal TRP120-TR binds the Notch-1 LBR.

180  
181 ***E. chaffeensis* TRP120-TR domain is required for Notch activation.** Both the N-terminal  
182 MNNL and cysteine-rich DSL domain of Notch ligands are known to be required for receptor  
183 binding; however, there is little known regarding ligand motifs required for Notch activation. We  
184 have previously demonstrated Notch activation occurs in THP-1 cells after stimulation with  
185 TRP120-coated beads for 15 min (6). Gene expression levels of *notch1*, *hes1* and *hes5* were  
186 upregulated after incubation with TRP120-coated beads. To further delineate the TRP120  
187 domain required for Notch activation THP-1 cells or primary human monocytes were treated  
188 with soluble purified full length or truncated constructs of recombinant TRP120 (rTRP120-TR  
189 and -C-terminus) (Figs. S2A-B). Full length rTRP120 and rTRP120-TR caused NICD nuclear  
190 translocation 2 h post-treatment (Figs. 3A-B). NICD nuclear translocation was not observed in  
191 untreated cells, cells treated with TRX or rTRP120-C-terminal soluble proteins (Figs. 3A-B).  
192 Collectively, these data demonstrate the requirement of TRP120-TR for Notch activation.

193  
194 ***E. chaffeensis* TRP120-TR Notch ligand IDD-mimetic activates Notch.**  
195 To determine if Notch is activated by a TRP120-TR Notch mimetic IDD motif, several TRP120-  
196 TR synthetic peptides were generated (Fig. 4A). THP-1 cells or primary human monocytes were  
197 treated with TRP120-TR IDD peptides or scrambled negative control peptide for 2 h. A 35-aa  
198 TRP120-TR IDD motif (TRP120-N1-P3) caused nuclear translocation (Figs. 4B and C).  
199 Importantly, the identified IDD contained a motif identified in both sequence homology and ISM  
200 data (Fig. 1C). Inhibition of Notch signaling by DAPT, a  $\gamma$ -secretase inhibitor, abrogated Notch  
201 activation with TRP120-N1-P3 treatment, indicating that TRP120-N1-P3 directly binds to the  
202 Notch-1 receptor for Notch activation (Fig. 4B). To confirm Notch activation by TRP120-N1-P3,

203 gene expression levels of Notch downstream targets were examined by human Notch signaling  
204 pathway array analysis. In comparison to untreated THP-1 cells, a significant increase in Notch  
205 downstream targets, including HES1, HES5, HEY1 and HEY2 gene expression levels occurred  
206 in TRP120-N1-P3 treated cells (Figs. 5A-B, Table S1A). Interestingly, Notch gene expression by  
207 TRP120-N1-P3 treatment was increased in a concentration-dependent manner (Fig. 5B, Table  
208 S1A). Importantly, rJagged-1 also demonstrated similar upregulation of Notch genes in a  
209 concentration-dependent manner (Fig. S3). These data demonstrate that a TRP120 IDD  
210 mimetic motif is responsible for TRP120 Notch activation.

211

### 212 ***E. chaffeensis* TRP120-TR Notch ligand SLiM mimetic activates Notch.**

213 It is well-documented that SLiMs are found in two general groups; posttranslational modification  
214 (PTM) motifs or ligand motifs that mediate binding events. We have previously identified a  
215 functional TRP120 HECT E3 ligase catalytic motif located in the C-terminus (2, 7) and have  
216 recently identified a TRP120-TR Wnt SLiM mimetic motif (3). To determine if the TRP120-TR  
217 Notch mimetic motif could be a SLiM (3-12 aa), overlapping TRP120-TR synthetic peptides that  
218 span the identified 35-aa TRP120-TR IDD motif were synthesized (Fig. 6A). Treatment with P4  
219 and P5 TRP120-TR Notch mimetic SLiM peptides in THP-1 cells did not result in NICD nuclear  
220 translocation (Fig. 6B); however, TRP120-TR Notch mimetic SLiM P6 (TRP120-N1-P6) located  
221 at the C-terminus resulted in NICD nuclear translocation (Fig. 6B). TRP120-N1-P6 was also  
222 shown to cause NICD nuclear translocation in primary human monocytes (Fig. 6C).  
223 Furthermore, pre-treatment of DAPT inhibited TRP120-N1-P6 Notch activation (Fig. 6B).  
224 Upregulation of Notch downstream targets occurred with TRP120-N1-P6 treatment in a  
225 concentration dependent manner (Figs. 7A-B, Table S1B), as previously shown with the  
226 TRP120-N1-P3 peptide. In comparison, TRP120-N1-P5 peptide treatment, did not result in  
227 significant upregulation of Notch gene expression (Fig. 7B).

228 To confirm that TRP120-N1-P6 is required for Notch activation, a TRP120-N1-P3 mutant  
229 peptide (dmut) (Fig. 6A) without the TRP120-N1-P6 motif was tested. THP-1 cells stimulated  
230 with TRP120-N1-dmut exhibited abrogated Notch activation as demonstrated by NICD  
231 translocation (Fig. 6B). To determine the minimal residues required in the TRP120-TR Notch  
232 mimetic SLiM, alanine mutagenesis was used to determine the contribution of specific residues  
233 to Notch activation (Fig. 8A, blue boxes). Mutated residues were selected based on sequence  
234 homology and ISM data. Mutants (dmut-1 -2, -3 and -4) exhibited reduced Notch activation as  
235 determined by NICD translocation, but only the TRP120-N1-dmut peptide resulted in full  
236 abrogation of NICD nuclear translocation (Fig. 8A). Collectively, these data demonstrate that the  
237 TRP120-N1-P6 SLiM is a Notch mimetic.

238

239 **TRP120 Notch SLiM antibody blocks *E. chaffeensis* Notch activation.** To investigate  
240 whether the TRP120 Notch mimetic is solely responsible for Notch activation by *E. chaffeensis*,  
241 THP-1 cells were pre-treated with a purified rabbit polyclonal antibody generated against the  
242 TRP120-N1-P6 SLiM and subsequently infected with *E. chaffeensis* for 2 h. Negative pre-  
243 immune serum was used as a negative control. NICD nuclear translocation was determined in  
244  $\alpha$ -TRP120-N1-P6 SLiM or negative pre-immune serum treated cells. THP-1 cells treated with  $\alpha$ -  
245 TRP120-N1-P6 SLiM did not display NICD nuclear translocation, in comparison to the negative  
246 pre-immune serum control (Fig. 8B). These data suggests that TRP120-N1-P6 SLiM is the only  
247 Notch mimic involved in Notch activation by *E. chaffeensis*.

248

## 249 Discussion

250 We have previously demonstrated TRP120-host interactions to occur with a diverse  
251 array of host cell proteins associated with conserved signaling pathways, including Wnt and  
252 Notch (8). Two proteins shown to interact with TRP120 were the Notch metalloprotease, a  
253 disintegrin and metalloprotease domain (ADAM17), and a Notch antagonist, F-box and WD

254 repeat domain-containing 7 (FBW7). In addition, we have demonstrated that secretion of *E.*  
255 *chaffeensis* TRP120 activates Notch signaling to downregulate TLR2/4 expression for  
256 intracellular survival. Moreover, Keewan et al, demonstrated upregulation of Notch-1, IL-6 and  
257 MCL-1 during *M. avium paratuberculosis* infection (37). Notch-1 signaling was shown to  
258 modulate macrophage polarization and immune defense against during infection, but the  
259 molecular mechanisms were not defined; however, the molecular mechanisms utilized for  
260 TRP120 Notch activation have not been previously studied (6). In this study, we investigated the  
261 molecular interactions involved in TRP120 Notch activation and have defined a TRP120 Notch  
262 SLiM mimetic responsible for Notch activation.

263 Molecular mimicry has been well-established as an evolutionary survival strategy utilized  
264 by pathogens to disrupt or co-opt host function as a protective mechanism to avoid elimination  
265 by the host immune system (30, 32-36). More specifically, SLiMs are a distinct, intrinsically  
266 disordered class of protein interaction motifs that have been shown to evolve *de novo* for  
267 promiscuous binding to various partners and have been documented as a host hijacking  
268 mechanism for pathogens (26, 29, 30). Although SLiM mimicry has been established as a  
269 mechanism utilized by pathogens to repurpose host cell functions for survival, a Notch ligand  
270 mimic has never been defined.

271 TRP120 contains four intrinsically disordered tandem repeat (TR) domains that have  
272 been previously described as important for TRP120's moonlighting capabilities (9, 12). Within  
273 these intrinsically disordered domains are various SLiMs responsible for TRP120 multi-  
274 functionality. We have recently defined a novel TRP120 repetitive SLiM that activates Wnt  
275 signaling to promote *E. chaffeensis* infection (3). In the current study, we have also determined  
276 TRP120-TR as the domain also responsible for Notch activation. Sequence homology studies  
277 and Information Spectrum Method (ISM) have shown sequence similarity and similar biological  
278 function between TRP120 and endogenous Notch ligands. ISM is a virtual spectroscopy method

279 utilized to predict if proteins share a similar biological function based on the electron-ion  
280 interaction potential of amino acids, and only requires the nucleotide sequence of each protein.  
281 It was recently used to determine prediction of potential receptor, natural reservoir, tropism and  
282 therapeutic/vaccine target of SARS-CoV-2 (38). Our results demonstrate a shared sequence  
283 similarity and biological function with both canonical and non-canonical Notch ligands that  
284 occurs within the tandem repeat domain of TRP120 (TRP120-TR). Both sequence homology  
285 and ISM studies identified specific tandem repeat sequences that are functionally associated  
286 with endogenous Notch ligands and range between 20-35 amino acids in size. This data  
287 suggested that intrinsically disordered regions found within the TRP120-TR domain are  
288 responsible for Notch ligand mimic function and direct effector-host protein interaction with the  
289 Notch receptor.

290 Notch ligand binding occurs specifically with EGFs 11-13 within the LBR of the Notch  
291 receptor (39, 40). Canonical Notch ligands are known to contain a DSL domain that is important  
292 for Notch binding and activation, but a conserved activation motif has not been defined.  
293 Colocalization of TRP120 with Notch-1 was previously shown to occur during *E. chaffeensis*  
294 infection (6); however, a direct interaction was not previously shown using yeast-two hybrid (8),  
295 possibly due to limitations of this technique with protein interactions involving membrane  
296 proteins (6, 41). Using pull down, SPR and protein-coated fluorescent microsphere approaches,  
297 we further studied TRP120-Notch-1 interaction and found direct binding occurs through  
298 TRP120-TR at a Notch-1 LBR (EGFs 1-15). TRP120-TR and Notch-1 LBR interaction occurred  
299 at an affinity of  $120 \pm 2.0$  nM, indicating a strong protein-protein interaction. Numerous structural  
300 studies of interactions of Notch with endogenous ligands have shown low affinity interactions  
301 between Notch Jag or DLL ECDs (42-44). One study demonstrated weak affinities between  
302 Notch-1 with an engineered high affinity Jag-1 variant ( $K_D = 5.4$   $\mu$ M) and DLL4 (12.8  $\mu$ M) (39).  
303 The higher binding affinity of TRP120-TR in comparison to canonical Notch ligands suggests

304 that the four tandemly repeated motifs folds in a structure that potentiates binding between  
305 TRP120 and Notch-1. In addition, stimulating THP-1 cells and primary monocytes with TRP120-  
306 TR resulted in NICD nuclear translocation, indicating that TRP120-TR is the TRP120 domain  
307 responsible for Notch activation. Interestingly, TRP120-Fzd5 interaction also occurred through  
308 the tandem repeat domain and supports our current findings that TRP120-host protein  
309 interactions occur within regions of the tandem repeat domain, likely due to its disordered nature  
310 (3).

311         Secreted and membrane-bound proteins have been shown to activate Notch signaling.  
312 These non-canonical Notch ligands lack the DSL domain but still have the ability to modify  
313 Notch signaling. Some of the non-canonical Notch proteins contain EGF-like domains; however,  
314 others share very little sequence similarity to endogenous Notch ligands (23, 45). TSP2 is a  
315 secreted mammalian protein containing EGF-like domains. TSP2 was found to potentiate Notch  
316 signaling by direct Notch-3/Jagged1 binding (46). Furthermore, TSP2 binds directly to purified  
317 Notch-3 protein containing EGF-like domains 1–11, suggesting a direct interaction. Non-  
318 canonical Notch ligand TSP2 was found to share significant sequence homology within the  
319 TRP120-TR sequence. Homologous regions included the identified TRP120-TR Notch SLIM  
320 mimetic. Although TSP2 has been identified as a secreted, non-canonical Notch ligand, there  
321 has been no activating motif identified to date. F3/contactin1, another identified secreted non-  
322 canonical Notch ligand, does not contain DSL or EGF-like domains; however, it activates the  
323 Notch signaling pathway through the Notch-1 receptor (47). TRP120 was found to share  
324 biological function with F3/contactin1 by ISM. F3/contactin1 has been demonstrated to bind to  
325 Notch-1 at two different locations within the NECD and activates Notch signaling when  
326 presented as purified soluble protein (47). Therefore, Notch activation by secreted, non-  
327 canonical Notch ligands has been demonstrated; however, more insight into the molecular



328 details of those interactions needs to be elucidated. This study provides new insight regarding  
329 non-canonical Notch ligand activation of the Notch signaling pathway.

330 SLiMs have been identified in secreted effector proteins of intracellular bacterial  
331 pathogens, including *Ehrlichia*, *Anaplasma phagocytophilum* (48), *Legionella pneumophila* (49-  
332 51) and *Mycobacterium tuberculosis* (52). This investigation identifies a novel Notch SLiM (11  
333 aa) that can activate Notch signaling as a soluble ligand. Complete NICD nuclear translocation  
334 was previously shown to occur at 2 h post-infection (6), indicating that NICD nuclear  
335 translocation during *E. chaffeensis* infection is a result of TRP120-TR Notch ligand SLiM  
336 mimetic interaction with the Notch-1 receptor. In addition, Notch signaling pathway genes were  
337 upregulated at 24 h in TRP120-TR Notch mimetic SLiM-treated THP-1 cells. These data are  
338 consistent with our previous findings where we detected upregulation of Notch signaling  
339 pathway components and target genes during *E. chaffeensis* infection at 12, 24, 48, and 72  
340 h.p.i., with maximum changes in Notch gene expression occurring at 24 h.p.i (6). Furthermore,  
341 during *E. chaffeensis* infection, TRP120 mediated ubiquitination and proteasomal degradation of  
342 Notch negative regulator, FBW7 begins at 24 h.p.i. and gradually decreases during late stages  
343 of infection (2). Both TRP120 and FBW7 are localized to the nucleus beginning at 24 h.p.i.,  
344 suggesting that TRP120-degradadtion of FBW7 assists in upregulation of Notch downstream  
345 targets at this timepoint (2).

346 Interestingly, both the TRP120 Notch memetic IDD (TRP120-N1-P3) and SLiM  
347 (TRP120-N1-P6) resulted in concentration-dependent upregulation of Notch downstream  
348 targets. Similar to our findings, studies have shown that the Notch pathway can induce  
349 heterogenous phenotypic responses in a Notch ligand or NICD dose dependent manner. Klein  
350 et al. demonstrated that high levels of Notch ligands can induce a ligand inhibitory effect, while  
351 lower levels of Notch ligand activate Notch signaling activity (53). Similarly, Semenova D et al.  
352 has shown that NICD and Jag1 transduction increases osteogenic differentiation in a dose-

353 dependent manner; however high dosage of NICD and Jag1 decreases osteogenic  
354 differentiation efficiency (54). Furthermore, Gomez-Lamarca et al. has shown that NICD dosage  
355 can influence CSL-DNA binding kinetics, NICD dimerization, and chromatin opening to  
356 strengthen transcriptional activation (55). Therefore, an increase in Notch ligand-receptor  
357 interaction may lead to increased NICD release and Notch signaling strength.

358 Alanine mutagenesis demonstrated the entire 11-aa TRP120-TR Notch ligand SLiM  
359 mimetic is required for Notch activation. Importantly, SLiMs are known to have low-affinity,  
360 transient protein-protein interactions within the low-micromolar range (26). In this case, the  
361 repeated TRP120-TR Notch ligand SLiM mimetic motif may cause TRP120 to fold in a tertiary  
362 structure upon binding to the Notch-1 receptor that stabilizes the TRP120-Notch-1 interaction.  
363 Based on this data, *E. chaffeensis* TRP120 could be used as a model to study SLiMs within  
364 intrinsically disordered effector proteins that are utilized for host exploitation by other  
365 intracellular bacterial pathogens.

366 To demonstrate that TRP120-TR Notch ligand SLiM mimetic motif is solely responsible  
367 for *E. chaffeensis* activation of Notch, we generated an antibody against the mimetic epitope to  
368 block *E. chaffeensis* TRP120-Notch-1 binding. Our results demonstrated antibody blockade of  
369 Notch activation by *E. chaffeensis*, rTRP120 and the TRP120-TR Notch ligand SLiM peptide.  
370 This data strongly supports the conclusion that the TRP120-TR Notch ligand SLiM mimetic is  
371 responsible for *E. chaffeensis* Notch activation and may provide a new *E. chaffeensis*  
372 therapeutic target. Hence, this study serves to provide insight into the molecular details of how  
373 Notch signaling is modulated during *E. chaffeensis* infection and may serve as a model for other  
374 pathogens.

375 Further outstanding questions regarding regulation of the Notch signaling pathway  
376 during *E. chaffeensis* remain. We have recently demonstrated maintenance of Notch activation  
377 is linked to TRP120-mediated ubiquitination and proteasomal degradation of tumor suppressor

378 FBW7, a Notch negative regulator (2). However, other potential Notch regulators may serve as  
379 a target for TRP120-mediated ubiquitination for constitutive Notch activation during infection.  
380 Suppressor of Deltex [Su(dx)] is an E3 ubiquitin ligase that serves as another negative regulator  
381 of Notch signaling by degrading Deltex, a positive regulator of Notch signaling (56). Su(dx) may  
382 serve as another target of TRP120-mediated ubiquitination to maintain Notch activity during *E.*  
383 *chaffeensis* infection. Furthermore, how secreted non-canonical Notch ligands are able to cause  
384 separation between the NICD and NECD remains unknown. TRP120 causes Notch activation,  
385 resulting in upregulation of Notch downstream targets; however, the mechanism of how the S2  
386 exposure for ADAM cleavage is not understood. Future crystallography studies on TRP120 and  
387 Notch-1 interaction may provide more insight into these structural details required for TRP120-  
388 N1-P6 SLiM Notch activation (57, 58).

389 In conclusion, we have demonstrated *E. chaffeensis* Notch activation is initiated by a  
390 TRP120 Notch SLiM mimetic. Our findings have identified a pathogen protein host mimic to  
391 repurpose the evolutionarily conserved Notch signaling pathway for intracellular survival. This  
392 study gives more insight into how obligate intracellular pathogens, with small genomes have  
393 evolved host mimicry modules *de novo* to exploit conserved signaling pathways to suppress  
394 innate defenses to promote infection.

395

## 396 **Materials and Methods**

397 **Cell culture and cultivation of *E. chaffeensis*.** Human monocytic leukemia cells (THP-1;  
398 ATCC TIB-202) were propagated in RPMI media (ATCC) containing 2 mM L-glutamine, 10 mM  
399 HEPES, 1 mM sodium pyruvate, 4500 mg/L glucose, 1500 mg/L sodium bicarbonate,  
400 supplemented with 10% fetal bovine serum (FBS; Invitrogen) at 37°C in 5% CO<sub>2</sub> atmosphere. *E.*  
401 *chaffeensis* (Arkansas strain) was cultivated in THP-1 cells. Host cell-free *E. chaffeensis* was  
402 prepared by rupturing infected THP-1 cells or primary human monocytes with sterile glass

403 beads (1 mm) by vortexing. Infected THP-1 cells were harvested and pelleted by centrifugation  
404 at  $500 \times g$  for 5 min. The pellet was resuspended in sterile phosphate-buffered saline (PBS) in a  
405 50-ml tube containing glass beads and vortexed at moderate speed for 1 min. The cell debris  
406 was pelleted at  $1,500 \times g$  for 10 min, and the supernatant was further pelleted by high-speed  
407 centrifugation at  $12,000 \times g$  for 10 min,  $4^{\circ}\text{C}$ . The purified ehrlichiae were resuspended in fresh  
408 RPMI media and utilized as needed.

409 **Human PBMC and primary monocyte isolation.** Primary human monocytes were isolated  
410 from 125ml of human blood obtained from Gulf Coast Regional Blood Center (Houston, TX).  
411 Blood was diluted in RPMI media and separated by density gradient separation on Ficoll at  
412 2000rpm for 20 minutes. The plasma was removed from the separated sample and the buffy  
413 coat was collected. Buffy coat was diluted with DPBS containing 2% FBS and 1mM EDTA and  
414 centrifuged at 1500rpm for 15 minutes. Supernatant was removed and all cells were combined  
415 and mixed carefully. Combined cells were then centrifuged at 1500rpm for 10 minutes and  
416 supernatant was removed. Cells were resuspended into 1mL of DPBS containing 2% FBS and  
417 1mM EDTA. Cells were then diluted to  $5 \times 10^7/\text{mL}$  concentration, and monocytes were  
418 separated by the EasySep Human Monocyte Enrichment Kit w/o CD16 depletion (Stemcell  
419 #19058) according to the manufacturers protocol. Primary human monocytes were then cultured  
420 in RPMI media (ATCC) containing 2 mM L-glutamine, 10 mM HEPES, 1 mM sodium pyruvate,  
421 4500 mg/L glucose, 1500 mg/L sodium bicarbonate, supplemented with 10% fetal bovine serum  
422 (FBS; Invitrogen) at  $37^{\circ}\text{C}$  in 5%  $\text{CO}_2$  atmosphere.

423 **Antibodies and Reagents.** Primary antibodies used in this study for immunofluorescence  
424 microscopy, Western blot analysis, and pull-down assays include monoclonal rabbit  $\alpha$ -Notch1  
425 (3608S; Cell Signaling Technology, Danvers MA), polyclonal rabbit  $\alpha$ -Notch1, intracellular (07-  
426 1231; Millipore Sigma, Billerica, MA), rabbit  $\alpha$ -TRP120-I1 (59) polyclonal rabbit  $\alpha$ -TRX (T0803;  
427 Sigma-Aldrich, Saint Louis, MO). Polyclonal rabbit anti-TRP120 antiserum was commercially

428 generated against a TRP120 epitope inclusive of aa. 290-301 (GenScript, Piscataway, NJ).

429 Synthetic peptides used in this study were commercially generated (Genscript, Piscataway, NJ).

430 **Sequence Homology.** Genome and transcriptome sequences encoding *E. chaffeensis* TRP120  
431 and *Homo sapiens* Notch ligand proteins were recovered using BLAST searches with the online  
432 version at the NCBI website. Sequences were submitted to NCBI Protein BLAST and ClustalW2  
433 sequence databases for sequence alignment.

434 **Informational Spectrum Method (ISM).** ISM analyzes the primary structure of proteins by  
435 assigning a physical parameter which is relevant for the protein's biological function (38, 60).  
436 Each amino acid in TRP120 and Notch ligand sequences was given a value corresponding to its  
437 electron-ion interaction potential (EIIP), which determines the long-range properties of biological  
438 molecules. The value of the amino acids within the protein were Fourier transformed to provide  
439 a Fourier spectrum that is representative of the protein, resulting in a series of frequencies and  
440 amplitudes. The frequencies correspond to a physico-chemical property involved in the  
441 biological activity of the protein. Comparison of proteins is performed by cross-spectra analysis.  
442 Proteins with similar spectra were predicted to have a similar biological function. Inverse Fourier  
443 Transform was performed to identify the sequence responsible for obtained signals at a given  
444 frequency.

445 **Transfection.** HeLa cells ( $1 \times 10^6$ ) were seeded in a 60 mm culture dish 24 h prior to  
446 transfection. AcGFP-TRP120 or AcGFP-control plasmids were added to OptiMem and  
447 Lipofectamine 2000 mixture and incubated for 20 min at 37°C. Lipofectamine/plasmid mixtures  
448 were added to HeLa cells and incubated for 4 h at 37°C. Media was aspirated 4 h post-  
449 transfection and fresh media was added to each plate and incubated for 24 h.

450 **Pull Down Assay.** Recombinant His-tagged TRP120 (10 µg) and Notch-1 (10 µg) (Sino  
451 Biological) were incubated with Ni-NTA beads alone, or in combination, for 4 h at 4°C.

452 Supernatants were collected and the Ni-NTA beads were washed 5X with 10 mM imidazole  
453 wash buffer. Proteins were eluted off with 200 mM imidazole elution buffer and binding  
454 determined by Western blot analysis.

455 **Immunofluorescent Confocal Microscopy.** THP-1 cells ( $2 \times 10^6$ ) were treated with full length  
456 or truncated constructs (-TR or -C terminus) of recombinant TRP120, or TRP120 peptides for 2  
457 h at 37°C. Cells were collected and fixed using 4% formaldehyde, washed with 1X PBS and  
458 permeabilized and blocked in 0.5% Triton X-100 and 2% BSA in PBS for 30 min. Cells were  
459 washed with PBS and probed with polyclonal rabbit  $\alpha$ -Notch-1, intracellular (1:100) (Millipore  
460 Sigma, MA) or monoclonal rabbit  $\alpha$ -Notch1 (3608S; Cell Signaling Technology, Danvers MA) for  
461 1 h at room temperature. Cells were washed with PBS and probed with Alexa Fluor 568 rabbit  
462 anti-goat IgG (H+L) for 30 min at room temperature, washed and then mounted with ProLong  
463 Gold antifade reagent with DAPI (Molecular Probes, OR). Slides were imaged on a Zeiss LSM  
464 880 confocal laser scanning microscopy. Pearson's correlation coefficient and Mander's  
465 correlation coefficient was generated by ImageJ software to quantify the degree of  
466 colocalization between fluorophores.

467 **Protein-coated fluorescent microsphere assay.** TRP120 and TRX recombinant proteins were  
468 desalted using Zeba spin desalting columns (Thermo Fisher Scientific, MA) as indicated by the  
469 manufacturer protocol. Protein abundance of desalted recombinant protein was assessed by  
470 bicinchoninic acid assay (BCA assay). One-micrometer, yellow-green (505/515), sulfate  
471 FluoSpheres (Life Technologies, CA) were first equilibrated with 40 $\mu$ M of MES buffer followed  
472 by incubation with 10 $\mu$ g of desalted TRP120 or TRX recombinant protein in 40 $\mu$ M MES (2-(N-  
473 morpholino) ethanesulfonic acid) buffer for 2 h at room temperature on a rotor. TRP120 or TRX  
474 coated FluoSpheres were washed twice with 40 $\mu$ M MES buffer at 12,000 x g for 5 mins and  
475 then resuspended in RPMI media. To determine TRP120 or TRX protein coating of  
476 FluoSpheres, dot blotting of FluoSpheres samples was performed after protein coating using  $\alpha$ -

477 TRX or  $\alpha$ -TRP120 antibodies.  $8 \times 10^5$  THP-1 cells/well were plated in a 96-well round bottom  
478 plate, and the TRP120 or TRX coated FluoSpheres were added to each well at approximately 5  
479 beads/cell. The cell and protein-coated FluoSpheres were incubated between 5-60 mins at 37°C  
480 with 5% CO<sub>2</sub>, collected and unbound beads were washed twice with 1 X PBS, followed by  
481 fixation by cytopspin for 15 mins. Cell samples were then processed for analysis by  
482 immunofluorescent confocal microscopy, as previously mentioned. FluoSpheres are light-  
483 sensitive, therefore all steps were performed in the dark.

484 **Quantitative Real-time PCR.** The human Notch signaling targets PCR array profiles the  
485 expression of 84 Notch pathway-focused genes to analyze Notch pathway status. PCR arrays  
486 were performed according to the PCR array handbook from the manufacturer. Briefly,  
487 uninfected and *E. chaffeensis*-infected or Notch mimetic peptide-treated THP-1 cells were  
488 collected at 24 and 48 h intervals and RNA purification with minor modifications, cDNA  
489 synthesis and real-time PCR were performed as previously described (3).

490 **Western Blot Analysis.** Cells were lysed in RIPA lysis buffer (0.5M Tris-HCl, pH 7.4, 1.5M  
491 NaCl, 2.5% deoxycholic acid, 10% NP-40, 10mM EDTA) containing protease inhibitor cocktail  
492 for 30 min at 4°C. Lysates were then cleared by centrifugation and protein abundance assessed  
493 by bicinchoninic acid assay (BCA assay). Samples were added to Laemelli buffer then boiled for  
494 5 min. Lysates were then subjected to SDS-PAGE followed by transfer to nitrocellulose  
495 membrane. Membranes were blocked for 1 h in 5% nonfat milk diluted in TBST and then  
496 exposed to  $\alpha$ -TRP120,  $\alpha$ -TRX or  $\alpha$ -Notch-1 primary antibodies overnight. Membranes were  
497 washed three times in Tris-buffered saline containing 1% Triton (TBST) for 30 min followed by 1  
498 h incubation with horseradish peroxidase-conjugated anti-rabbit and anti-mouse secondary  
499 antibodies (SeraCare, Milford, MA) (diluted 1:10,000 in 5% nonfat milk in TBST). Proteins were  
500 visualized with ECL via Chemi-doc2 and densitometry was measured with VisionWorks Image  
501 Acquisition and Analysis Software.

502 **Surface Plasmon Resonance.** SPR was performed using a BIAcore T100 instrument with  
503 nitrilotriacetic acid (NTA) sensor chip. Purified polyhistidine-tagged, full-length, rTRP120-TR,  
504 rTRX and human rNotch-1 Fc Chimera Protein, CF (R&D Systems, MN) were dialyzed in  
505 running buffer (100 mM sodium phosphate [pH 7.4], 400 mM NaCl, 40  $\mu$ M EDTA, 0.005%  
506 [vol/vol]). Briefly, each cycle of running started with charging the NTA chip with 500  $\mu$ M of NiCl<sub>2</sub>.  
507 Subsequently, purified polyhistidine-tagged, full-length, truncated rTRP120 proteins, or rTRX  
508 (0.1  $\mu$ M) were immobilized on the NTA sensor as ligand on flow cell 2. Immobilization was  
509 carried out at 25°C at a constant flow rate of 30  $\mu$ l/min for 100s. Varying concentrations of  
510 Notch1-NECD constructs (0-800 nM) were injected over sensor surfaces as analyte with  
511 duplicates along with several blanks of running buffer. Injections of analyte were carried out at a  
512 flow rate of 30  $\mu$ l/min with contact time of 360 s and a dissociation time of 300 s. Finally, the  
513 NTA surface was regenerated by using 350 mM EDTA. Readout included a sensogram plot of  
514 response against time, showing the progress of the interaction. Curve fittings were done with  
515 the 1:1 Langmuir binding model with all fitting quality critique requirements met. The binding  
516 affinity ( $K_D$ ) was determined for all interactions by extracting the association rate constant and  
517 dissociation rate constant from the sensorgram curve ( $K_D = K_d/K_a$ ) using the BIAevaluation  
518 package software.

519 **TRP120 Antibody Inhibition of *E. chaffeensis* Notch activation.** Host cell-free *E. chaffeensis*  
520 was pre-treated with 5-10  $\mu$ g/ml of polyclonal rabbit anti-TRP120 antibody generated against the  
521 TRP120 Notch mimetic SLiM (aa. 284-301), or purified IgG antibody. The cell-free *E.*  
522 *chaffeensis*/antibody mixture was then added to THP-1 cells ( $5 \times 10^5$ ) in a 12-well plate for 2 h.  
523 Samples were collected, washed with PBS and prepared for IFA.

524 **TRP120 Protein Expression and Purification.** Full length or truncated constructs of rTRP120,  
525 or rTRX control were expressed in a pBAD expression vector, which has been previously  
526 optimized by our laboratory (59, 61, 62). Recombinant TRP120 full length, truncated constructs,



527 and rTRX were purified via nickel-nitrilotriacetic acid (Ni-NTA) purification system. All  
528 recombinant proteins were dialyzed via PBS and tested for bacterial endotoxins using the  
529 Limulus Amebocyte Lysate (LAL) test.

530 **Statistical Analysis.** All data are represented as the means  $\pm$  standard deviation (SD) of data  
531 obtained from at least three independent experiments done with triplicate biological replicates,  
532 unless otherwise indicated. Analyses were performed using a two-way ANOVA or two-tailed  
533 Student's *t*-test (GraphPad Prism 6 software, La Jolla, CA). A P-value of  $<0.05$  was considered  
534 statistically significant.

535 **Acknowledgments**

536 We thank the UTMB Solution Biophysics Laboratory and the Optical Microscopy Core for  
537 assistance with confocal microscopy. This work was supported by the National Institute of  
538 Allergy and Infectious Diseases grants AI158422, AI149136 and AI126144 to J.W.M., a UTMB  
539 McLaughlin Endowment Predoctoral Fellowship to L.L.P., an NIH 1F31AI152424 fellowship to  
540 L.L.P., and a T32AI007526-20 biodefense training fellowship to C.D.B.

541 **References**

- 542 1. Jaworski DC, Cheng C, Nair ADS, Ganta RR. 2017. *Amblyomma americanum* ticks  
543 infected with in vitro cultured wild-type and mutants of *Ehrlichia chaffeensis* are  
544 competent to produce infection in naive deer and dogs. *Ticks Tick Borne Dis* 8:60-64.
- 545 2. Wang JY, Zhu B, Patterson LL, Rogan MR, Kibler CE, McBride JW. 2020. *Ehrlichia*  
546 *chaffeensis* TRP120-mediated ubiquitination and proteasomal degradation of tumor  
547 suppressor FBW7 increases oncoprotein stability and promotes infection. *PLoS Pathog*  
548 16:e1008541.
- 549 3. Rogan MR, Patterson LL, Byerly CD, Luo T, Paessler S, Veljkovic V, Quade B, McBride  
550 JW. 2021. *Ehrlichia chaffeensis* TRP120 Is a Wnt Ligand Mimetic That Interacts with  
551 Wnt Receptors and Contains a Novel Repetitive Short Linear Motif That Activates Wnt  
552 Signaling. *mSphere* 6.
- 553 4. Luo T, Dunphy PS, Lina TT, McBride JW. 2015. *Ehrlichia chaffeensis* exploits canonical  
554 and noncanonical host Wnt signaling pathways to stimulate phagocytosis and promote  
555 intracellular survival. *Infect Immun* 84:686-700.
- 556 5. Lina TT, Luo T, Velayutham TS, Das S, McBride JW. 2017. *Ehrlichia* activation of Wnt-  
557 PI3K-mTOR signaling inhibits autolysosome generation and autophagic destruction by  
558 the mononuclear phagocyte. *Infect Immun* 85.
- 559 6. Lina TT, Dunphy PS, Luo T, McBride JW. 2016. *Ehrlichia chaffeensis* TRP120 activates  
560 canonical Notch signaling to downregulate TLR2/4 expression and promote intracellular  
561 survival. *MBio* 7.
- 562 7. Zhu B, Das S, Mitra S, Farris TR, McBride JW. 2017. *Ehrlichia chaffeensis* TRP120  
563 moonlights as a HECT E3 ligase involved in self and host ubiquitination to influence  
564 protein interactions and stability for intracellular survival. *Infect Immun*  
565 doi:10.1128/IAI.00290-17.
- 566 8. Luo T, Kuriakose JA, Zhu B, Wakeel A, McBride JW. 2011. *Ehrlichia chaffeensis*  
567 TRP120 interacts with a diverse array of eukaryotic proteins involved in transcription,  
568 signaling, and cytoskeleton organization. *Infect Immun* 79:4382-91.
- 569 9. Klema VJ, Sepuru KM, Fullbrunn N, Farris TR, Dunphy PS, McBride JW, Rajarathnam  
570 K, Choi KH. 2018. *Ehrlichia chaffeensis* TRP120 nucleomodulin binds DNA with  
571 disordered tandem repeat domain. *PLoS One* 13:e0194891.
- 572 10. Zhu B, Kuriakose JA, Luo T, Ballesteros E, Gupta S, Fofanov Y, McBride JW. 2011.  
573 *Ehrlichia chaffeensis* TRP120 binds a G+C-rich motif in host cell DNA and exhibits  
574 eukaryotic transcriptional activator function. *Infect Immun* 79:4370-81.
- 575 11. Mitra S, Dunphy PS, Das S, Zhu B, Luo T, McBride JW. 2018. *Ehrlichia chaffeensis*  
576 TRP120 effector targets and recruits host polycomb group proteins for degradation to  
577 promote intracellular infection. *Infect Immun* 86.
- 578 12. Byerly CD, Patterson LL, McBride JW. 2021. *Ehrlichia* TRP effectors: moonlighting,  
579 mimicry and infection. *Pathog Dis* 79.
- 580 13. Baonza A, Garcia-Bellido A. 2000. Notch signaling directly controls cell proliferation in  
581 the *Drosophila* wing disc. *Proc Natl Acad Sci U S A* 97:2609-14.
- 582 14. Urbanek K, Lesiak M, Krakowian D, Koryciak-Komarska H, Likus W, Czekaj P, Kusz D,  
583 Sieron AL. 2017. Notch signaling pathway and gene expression profiles during early in  
584 vitro differentiation of liver-derived mesenchymal stromal cells to osteoblasts. *Lab Invest*  
585 97:1225-1234.
- 586 15. Zweidler-McKay PA, He Y, Xu L, Rodriguez CG, Karnell FG, Carpenter AC, Aster JC,  
587 Allman D, Pear WS. 2005. Notch signaling is a potent inducer of growth arrest and  
588 apoptosis in a wide range of B-cell malignancies. *Blood* 106:3898-906.
- 589 16. Artavanis-Tsakonas S, Rand MD, Lake RJ. 1999. Notch signaling: cell fate control and  
590 signal integration in development. *Science* 284:770-6.

- 591 17. Nakano N, Nishiyama C, Yagita H, Koyanagi A, Ogawa H, Okumura K. 2011. Notch1-  
592 mediated signaling induces MHC class II expression through activation of class II  
593 transactivator promoter III in mast cells. *J Biol Chem* 286:12042-8.
- 594 18. Hoyne GF. 2003. Notch signaling in the immune system. *J Leukoc Biol* 74:971-81.
- 595 19. Sarin A, Marcel N. 2017. The NOTCH1-autophagy interaction: Regulating self-eating for  
596 survival. *Autophagy* 13:446-447.
- 597 20. Palaga T, Ratanabunyong S, Pattarakankul T, Sangphech N, Wongchana W, Hadae Y,  
598 Kueanjinda P. 2013. Notch signaling regulates expression of Mcl-1 and apoptosis in  
599 PPD-treated macrophages. *Cell Mol Immunol* 10:444-52.
- 600 21. Miele L, Osborne B. 1999. Arbiter of differentiation and death: Notch signaling meets  
601 apoptosis. *J Cell Physiol* 181:393-409.
- 602 22. Chillakuri CR, Sheppard D, Lea SM, Handford PA. 2012. Notch receptor-ligand binding  
603 and activation: insights from molecular studies. *Semin Cell Dev Biol* 23:421-8.
- 604 23. D'Souza B, Miyamoto A, Weinmaster G. 2008. The many facets of Notch ligands.  
605 *Oncogene* 27:5148-67.
- 606 24. Edwards RJ, Davey NE, O'Brien K, Shields DC. 2012. Interactome-wide prediction of  
607 short, disordered protein interaction motifs in humans. *Mol Biosyst* 8:282-95.
- 608 25. Kumar M, Gouw M, Michael S, Samano-Sanchez H, Pancsa R, Glavina J, Diakogianni  
609 A, Valverde JA, Bukirova D, Calyseva J, Palopoli N, Davey NE, Chemes LB, Gibson TJ.  
610 2020. ELM-the eukaryotic linear motif resource in 2020. *Nucleic Acids Res* 48:D296-  
611 D306.
- 612 26. Van Roey K, Uyar B, Weatheritt RJ, Dinkel H, Seiler M, Budd A, Gibson TJ, Davey NE.  
613 2014. Short linear motifs: ubiquitous and functionally diverse protein interaction modules  
614 directing cell regulation. *Chem Rev* 114:6733-78.
- 615 27. Davey NE, Van Roey K, Weatheritt RJ, Toedt G, Uyar B, Altenberg B, Budd A, Diella F,  
616 Dinkel H, Gibson TJ. 2012. Attributes of short linear motifs. *Mol Biosyst* 8:268-81.
- 617 28. Dunphy PS, Luo T, McBride JW. 2014. *Ehrlichia chaffeensis* exploits host SUMOylation  
618 pathways to mediate effector-host interactions and promote intracellular survival. *Infect*  
619 *Immun* 82:4154-68.
- 620 29. Davey NE, Trave G, Gibson TJ. 2011. How viruses hijack cell regulation. *Trends*  
621 *Biochem Sci* 36:159-69.
- 622 30. Via A, Uyar B, Brun C, Zanzoni A. 2015. How pathogens use linear motifs to perturb  
623 host cell networks. *Trends Biochem Sci* 40:36-48.
- 624 31. Singh SB, Coffman CN, Carroll-Portillo A, Varga MG, Lin HC. 2021. Notch Signaling  
625 Pathway Is Activated by Sulfate Reducing Bacteria. *Front Cell Infect Microbiol*  
626 11:695299.
- 627 32. Drayman N, Glick Y, Ben-nun-shaul O, Zer H, Zlotnick A, Gerber D, Schueler-Furman O,  
628 Oppenheim A. 2013. Pathogens use structural mimicry of native host ligands as a  
629 mechanism for host receptor engagement. *Cell Host Microbe* 14:63-73.
- 630 33. Mondino S, Schmidt S, Buchrieser C. 2020. Molecular Mimicry: a Paradigm of Host-  
631 Microbe Coevolution Illustrated by Legionella. *mBio* 11.
- 632 34. Price CT, Al-Khodor S, Al-Quadan T, Santic M, Habyarimana F, Kalia A, Kwai YA.  
633 2009. Molecular mimicry by an F-box effector of Legionella pneumophila hijacks a  
634 conserved polyubiquitination machinery within macrophages and protozoa. *PLoS Pathog*  
635 5:e1000704.
- 636 35. Chemes LB, de Prat-Gay G, Sanchez IE. 2015. Convergent evolution and mimicry of  
637 protein linear motifs in host-pathogen interactions. *Curr Opin Struct Biol* 32:91-101.
- 638 36. Dunphy PS, Luo T, McBride JW. 2013. *Ehrlichia* moonlighting effectors and  
639 interkingdom interactions with the mononuclear phagocyte. *Microbes Infect* 15:1005-16.

- 640 37. Keewan E, Naser SA. 2020. Notch-1 Signaling Modulates Macrophage Polarization and  
641 Immune Defense against Mycobacterium avium paratuberculosis Infection in  
642 Inflammatory Diseases. *Microorganisms* 8.
- 643 38. Veljkovic V, Vergara-Alert J, Segales J, Paessler S. 2020. Use of the informational  
644 spectrum methodology for rapid biological analysis of the novel coronavirus 2019-nCoV:  
645 prediction of potential receptor, natural reservoir, tropism and therapeutic/vaccine target.  
646 *F1000Res* 9:52.
- 647 39. Luca VC, Kim BC, Ge C, Kakuda S, Wu D, Roein-Peikar M, Haltiwanger RS, Zhu C, Ha  
648 T, Garcia KC. 2017. Notch-Jagged complex structure implicates a catch bond in tuning  
649 ligand sensitivity. *Science* 355:1320-1324.
- 650 40. Whiteman P, de Madrid BH, Taylor P, Li D, Heslop R, Viticheep N, Tan JZ, Shimizu H,  
651 Callaghan J, Masiero M, Li JL, Banham AH, Harris AL, Lea SM, Redfield C, Baron M,  
652 Handford PA. 2013. Molecular basis for Jagged-1/Serrate ligand recognition by the  
653 Notch receptor. *J Biol Chem* 288:7305-12.
- 654 41. Bruckner A, Polge C, Lentze N, Auerbach D, Schlattner U. 2009. Yeast two-hybrid, a  
655 powerful tool for systems biology. *Int J Mol Sci* 10:2763-88.
- 656 42. Andrawes MB, Xu X, Liu H, Ficarro SB, Marto JA, Aster JC, Blacklow SC. 2013. Intrinsic  
657 selectivity of Notch 1 for Delta-like 4 over Delta-like 1. *J Biol Chem* 288:25477-25489.
- 658 43. Kershaw NJ, Church NL, Griffin MD, Luo CS, Adams TE, Burgess AW. 2015. Notch  
659 ligand delta-like1: X-ray crystal structure and binding affinity. *Biochem J* 468:159-66.
- 660 44. Cordle J, Johnson S, Tay JZ, Roversi P, Wilkin MB, de Madrid BH, Shimizu H, Jensen  
661 S, Whiteman P, Jin B, Redfield C, Baron M, Lea SM, Handford PA. 2008. A conserved  
662 face of the Jagged/Serrate DSL domain is involved in Notch trans-activation and cis-  
663 inhibition. *Nat Struct Mol Biol* 15:849-57.
- 664 45. Wang MM. 2011. Notch signaling and Notch signaling modifiers. *Int J Biochem Cell Biol*  
665 43:1550-62.
- 666 46. Meng H, Zhang X, Hankenson KD, Wang MM. 2009. Thrombospondin 2 potentiates  
667 notch3/jagged1 signaling. *J Biol Chem* 284:7866-74.
- 668 47. Hu QD, Ang BT, Karsak M, Hu WP, Cui XY, Duka T, Takeda Y, Chia W, Sankar N, Ng  
669 YK, Ling EA, Maciag T, Small D, Trifonova R, Kopan R, Okano H, Nakafuku M, Chiba S,  
670 Hirai H, Aster JC, Schachner M, Pallen CJ, Watanabe K, Xiao ZC. 2003. F3/contactin  
671 acts as a functional ligand for Notch during oligodendrocyte maturation. *Cell* 115:163-75.
- 672 48. Ijdo JW, Carlson AC, Kennedy EL. 2007. *Anaplasma phagocytophilum* AnkA is tyrosine-  
673 phosphorylated at EPIYA motifs and recruits SHP-1 during early infection. *Cell Microbiol*  
674 9:1284-1296.
- 675 49. Habyarimana F, Price CT, Santic M, Al-Khodori S, Kwaik YA. 2010. Molecular  
676 characterization of the Dot/Icm-translocated AnkH and AnkJ eukaryotic-like effectors of  
677 *Legionella pneumophila*. *Infect Immun* 78:1123-34.
- 678 50. Huang L, Boyd D, Amyot WM, Hempstead AD, Luo ZQ, O'Connor TJ, Chen C, Machner  
679 M, Montminy T, Isberg RR. 2011. The E Block motif is associated with *Legionella*  
680 *pneumophila* translocated substrates. *Cell Microbiol* 13:227-45.
- 681 51. Gomez-Valero L, Rusniok C, Cazalet C, Buchrieser C. 2011. Comparative and functional  
682 genomics of legionella identified eukaryotic like proteins as key players in host-pathogen  
683 interactions. *Front Microbiol* 2:208.
- 684 52. Ravi Chandra B, Gowthaman R, Akhouri RR, Gupta D, Sharma A. 2004. Distribution of  
685 proline-rich (PxxP) motifs in distinct proteomes: functional and therapeutic implications  
686 for malaria and tuberculosis. *Protein Eng Des Sel* 17:175-82.
- 687 53. Klein T, Brennan K, Arias AM. 1997. An intrinsic dominant negative activity of serrate  
688 that is modulated during wing development in *Drosophila*. *Dev Biol* 189:123-34.

- 689 54. Semenova D, Bogdanova M, Kostina A, Golovkin A, Kostareva A, Malashicheva A.  
690 2020. Dose-dependent mechanism of Notch action in promoting osteogenic  
691 differentiation of mesenchymal stem cells. *Cell Tissue Res* 379:169-179.
- 692 55. Gomez-Lamarca MJ, Falo-Sanjuan J, Stojnic R, Abdul Rehman S, Muresan L, Jones  
693 ML, Pillidge Z, Cerda-Moya G, Yuan Z, Baloul S, Valenti P, Bystricky K, Payre F,  
694 O'Holleran K, Kovall R, Bray SJ. 2018. Activation of the Notch Signaling Pathway In Vivo  
695 Elicits Changes in CSL Nuclear Dynamics. *Dev Cell* 44:611-623 e7.
- 696 56. Cornell M, Evans DA, Mann R, Fostier M, Flaszka M, Monthatong M, Artavanis-Tsakonas  
697 S, Baron M. 1999. The *Drosophila melanogaster* Suppressor of *deltex* gene, a regulator  
698 of the Notch receptor signaling pathway, is an E3 class ubiquitin ligase. *Genetics*  
699 152:567-76.
- 700 57. Hambleton S, Valeyev NV, Muranyi A, Knott V, Werner JM, McMichael AJ, Handford PA,  
701 Downing AK. 2004. Structural and functional properties of the human notch-1 ligand  
702 binding region. *Structure* 12:2173-83.
- 703 58. Maveyraud L, Mourey L. 2020. Protein X-ray Crystallography and Drug Discovery.  
704 *Molecules* 25.
- 705 59. Luo T, Zhang X, McBride JW. 2009. Major species-specific antibody epitopes of the  
706 *Ehrlichia chaffeensis* p120 and *E. canis* p140 orthologs in surface-exposed tandem  
707 repeat regions. *Clin Vaccine Immunol* 16:982-90.
- 708 60. Deng SP, Huang DS. 2014. SFAPS: an R package for structure/function analysis of  
709 protein sequences based on informational spectrum method. *Methods* 69:207-12.
- 710 61. Doyle CK, Nethery KA, Popov VL, McBride JW. 2006. Differentially expressed and  
711 secreted major immunoreactive protein orthologs of *Ehrlichia canis* and *E. chaffeensis*  
712 elicit early antibody responses to epitopes on glycosylated tandem repeats. *Infect*  
713 *Immun* 74:711-20.
- 714 62. Luo T, Zhang X, Wakeel A, Popov VL, McBride JW. 2008. A variable-length PCR target  
715 protein of *Ehrlichia chaffeensis* contains major species-specific antibody epitopes in  
716 acidic serine-rich tandem repeats. *Infect Immun* 76:1572-80.

717 **Figure Legends**

718 **Fig. 1. *E. chaffeensis* TRP120 shares sequence homology and biological function with**  
719 **canonical and noncanonical Notch ligands.** (A) BLAST analysis of TRP120 with  
720 canonical/noncanonical Notch ligands demonstrating amino acid homology. An asterisk (\*)  
721 represents identical conserved amino acid residues; a colon (:) represents conservative  
722 substitutions. (B) Informational Spectrum Method (ISM) was used to predict if TRP120 shared  
723 similar biological function with canonical and noncanonical Notch ligands. Primary sequences  
724 of TRP120 and Notch ligands were converted into a numerical sequence-based electron ion  
725 interaction potential (EIIP) of each amino acid. Numerical sequences were converted into a  
726 spectrum using Fourier transform. To determine if proteins shared a similar biological function  
727 and cross spectra analysis was performed and similar biological function is denoted by a peak  
728 at a frequency of F(0.288). (C) Schematic of TRP120 N- C- (gray) and TR domains (blue) with  
729 four highlighted repetitive TRP120 TR motifs that share sequence homology with Notch ligands.  
730 ISM sequence shown in panel B (underlined). (\*) represents a partial tandem repeat containing  
731 similar (EDDTVSQPSLE) but non identical sequence to highlighted sequence.

732

733 **Fig. 2. *E. chaffeensis* TRP120-TR interactions with the Notch receptor ligand binding**  
734 **region (LBR).** (A) HeLa cells transfected with TRP120-GFP (green) and probed for  
735 endogenous Notch-1 (red) demonstrate colocalization by immunofluorescent microscopy.  
736 Colocalization was quantitated by Pearson's and Mander's coefficient (-1 no colocalization; +1  
737 strong colocalization). (B and C) His-tag pull down assays demonstrating direct interaction  
738 between TRP120 and Notch-1. Recombinant Fc-tagged Notch-1 LBR was incubated with (B)  
739 TRP120-FL-His, (C) TRP120-TR-His or TRX-His negative control on Talon metal affinity resin.  
740 Bound Notch-1, TRP120-His,  $\alpha$ -TRP120 against a TR peptide or TRX-His were detected with  $\alpha$ -  
741 Notch-1,  $\alpha$ -TRP120 or  $\alpha$ -TRX antibodies. (D-F) Surface plasmon resonance of (D) TRP120-FL-  
742 His, (E) TRP120-TR-His or (F) TRX-His with Fc-tagged Notch-1 LBR on a Biacore T100 with a

743 series S Ni-nitrilotriacetic acid (NTA) sensor chip. TRP120-FL-His, TRP120-TR-His or TRX-His  
744 were immobilized on the NTA chip and 2-fold dilutions (800nM to 25nM) of Fc-tagged Notch-1  
745 LBR were used as analyte to determine binding affinity ( $K_D$ ). Sensograms and  $K_D$  are  
746 representative of data from triplicate experiments. (G) THP-1 cells were treated with rTRX- or  
747 rTRP120-FL-coated fluorescent microspheres for varying time points (5-60 mins). Colocalization  
748 was visualized by confocal immunofluorescent microscopy. Notch-1 was immunostained with  
749 tetramethylrhodamine isothiocyanate [TRITC] and TRP120-coated fluorescein isothiocyanate  
750 [FITC] auto-fluorescent microspheres. Nuclei were stained with DAPI (blue). White boxes  
751 indicate areas of colocalization measurements. Scale bar = 10  $\mu$ m. (H) Dot blot of PBS, TRX or  
752 TRP120-FL-coated microspheres probed with  $\alpha$ -TRX or  $\alpha$ -TRP120 antibodies, respectively.

753

754 **Fig. 3. TRP120-TR activates Notch and NICD nuclear translocation in primary human**  
755 **monocytes.** (A) Soluble recombinant TRP120-TR or -C terminal proteins (2  $\mu$ g/ml) were  
756 incubated with THP-1 cells for 2 h. Cells were collected and NICD localization determined by  
757 confocal immunofluorescent microscopy. Uninfected/untreated or recombinant TRX-treated  
758 THP-1 cells were used as negative controls. *E. chaffeensis*-infected or recombinant Jagged-1  
759 treated THP-1 cells were used as positive controls. NICD nuclear translocation was detected in  
760 *E. ch*-infected, TRP120-TR and Jagged-1 treated cells. (B) Primary human monocytes were  
761 treated with soluble TRP120-TR or recombinant TRX as described above and NICD nuclear  
762 translocation was detected in *E. chaffeensis*-infected and TRP120-TR-treated cells. End point  
763 analysis was performed as described in Fig. 2. Experiments were performed in triplicate and  
764 representative images are shown.

765

766 **Fig. 4. A TRP120-TR Notch-1 memetic IDD peptide stimulates NICD nuclear translocation.**  
767 (A) Overlapping TRP120-TR IDD peptide sequences (P1-P3) (B) THP-1 cells or (C) Primary  
768 human monocytes were incubated with synthetic TRP120-TR IDD peptides to determine the



769 TRP120-TR Notch-1 memetic motif responsible for Notch activation. TRP120-TR peptides were  
770 overlapping peptides spanning an entire TR domain. Cells were treated with peptide (1 µg/ml)  
771 for 2 h and confocal immunofluorescent microscopy was used to visualize NICD localization.  
772 NICD nuclear translocation denotes Notch activation. A scrambled peptide (Ctrl-p) was used as  
773 negative control and *E.ch.* infected cells were used as positive control. To determine if direct  
774 interaction of the TRP120-N1-P3 peptide and Notch receptor was necessary for Notch  
775 activation, THP-1 cells were pre-treated with DAPT, a γ-secretase inhibitor, and treated with  
776 TRP120-N1-P3 peptide for 2 h.

777

778 **Fig. 5. TRP120-N1-P3 IDD peptide stimulates Notch gene expression.** (A) Table of Notch  
779 pathway genes with corresponding fold-change displaying differential expression (up, down or  
780 no change) at 24 h p.t with 10 ng/ml of TRP120-N1-P3 peptide (B) Scatter plots of expression  
781 array analysis of 84 Notch signaling pathway genes to determine Notch gene expression 24 h  
782 after stimulation with 1 ng/ml (top), 10 ng/ml (middle) or 100 ng/ml (bottom) of TRP120-N1-P3  
783 peptide. Purple lines denote a 2-fold up or down regulation in comparison to control, and the  
784 black line denotes no change. Scatter plots are representative of three independent  
785 experiments (n = 3).

786

787 **Fig. 6. A TRP120-TR Notch-1 memetic SLiM peptide activates Notch signaling.** (A)  
788 TRP120-N1 SLiM (P4-P6) and mutant (dmut) peptide sequences. (B) THP-1 cells or (C) primary  
789 human monocytes were treated with synthetic TRP120-TR SLiM peptides to identify the  
790 TRP120-TR Notch-1 SLiM memetic motif. TRP120-TR peptides were SLiM peptides spanning  
791 the entire TRP120-N1-P3 peptide sequence. TRP120-N1-P3 mutant peptide (dmut) has a  
792 deletion of the TRP120-N1-P6 amino acids. Cells were treated with peptide (1 µg/ml) for 2 h and  
793 NICD localization visualized by confocal microscopy. TRP120-N1-P3 peptide was used as a  
794 positive control. To determine if direct interaction of the TRP120-N1-P6 peptide and Notch

795 receptor was necessary for Notch activation, THP-1 cells were pre-treated with DAPT, a  $\gamma$ -  
796 secretase inhibitor, and treated with TRP120-N1-P6 peptide for 2 h. Representative data of all  
797 experiments are shown (n = 3).

798

799 **Fig. 7. TRP120-N1-P6 SLiM Notch memetic peptide stimulates Notch gene expression.** (A)

800 Selected Notch pathway genes with corresponding fold-change displaying differential  
801 expression (up- and downregulation) at 24 h p.t with 10 ng/ml of TRP120-N1-P6 peptide. (B)  
802 Scatter plots of expression array analysis of 84 Notch signaling pathway genes to determine  
803 Notch gene expression with 1 ng/ml, 10 ng/ml, 100 ng/ml of TRP120-N1-P6 peptide or TRP120-  
804 N1-P5 treatment (10 ng/ml) compared to untreated cells (bottom) at 24 p.t. Purple lines denote  
805 a 2-fold up or down regulation in comparison to control, and the black lines denotes no change.  
806 Scatter plots are representative of three independent experiments (n = 3).

807

808 **Fig. 8. Amino acids critical to TRP120-N1-P6 memetic SLiM activity and anti-SLiM**

809 **antibody blocks Notch activation** (A) Critical amino acids of the TRP120-N1-P6 memetic  
810 SLiM determined by alanine mutagenesis (mutant peptide sequences are shown above the  
811 corresponding panel). THP-1 cells were treated with mutant peptides (dmut2, -3 and -4; 1  $\mu$ g/ml)  
812 for 2 h and confocal immunofluorescent microscopy was used to visualize NICD localization.  
813 NICD nuclear translocation denotes Notch activation. Peptide dmut was used as a negative  
814 control and TRP120-N1-P6 was used as a positive control. (B) Cell-free *E. chaffeensis*,  
815 rTRP120-FL or TRP120-N1-P6 were incubated with  $\alpha$ -TRP120-N1-P6 rabbit polyclonal antibody  
816 (5  $\mu$ g/ml) for 30 min. Preimmune serum was used as control antibody. THP-1 cells were  
817 subsequently inoculated with the cell-free *E. chaffeensis*/ $\alpha$ -TRP120-N1-P6 mixture for 2 h and  
818 confocal immunofluorescent microscopy was used to visualize NICD nuclear localization.  
819 Representative data of all experiments are shown (n = 3).

820

821 **Fig. 9. Proposed model of *E. chaffeensis* TRP120 Notch activation.** A TRP120-TR Notch  
822 SLiM memetic motif (TRP120-N1-P6; yellow highlight) binds the Notch-1 extracellular domain at  
823 a region containing the confirmed Notch ligand binding domain (LBD) to activate Notch  
824 signaling. TRP120-N1-P6 binding leads to NICD nuclear translocation and upregulation of  
825 Notch gene targets.

826

827 **Fig. S1. TRP120 shares biological function with canonical and noncanonical Notch**  
828 **ligands.** Informational Spectrum Method (ISM) was used to predict if TRP120 shared similar  
829 biological function with endogenous canonical and noncanonical Notch ligands. The primary  
830 sequence of TRP120 and endogenous Notch ligands were converted into a numerical sequence  
831 using each amino acids electron ion interaction potential (EIIP). Numerical sequences were  
832 converted into a spectrum using Fourier transform. To determine if proteins shared a similar  
833 biological function and cross spectra analysis was performed with TRP120 and Notch ligands  
834 individually. Similar biological function is denoted by a peak at a frequency of F(0.288). TRP120  
835 was predicted to share a similar biological function as canonical Notch ligands (A) DLL1, (B)  
836 DLL3 and (C) DLL4 and (D) noncanonical Notch ligand, F3 Contactin-1.

837

838 **Fig. S2. Purification of recombinant TRP120 proteins.** (A) Schematic of TRP120-FL, -TR  
839 and -C-terminus recombinant proteins. TRP120-TR is expressed and purified as two tandem  
840 repeat domains. (B) Coomassie Blue stained gel displaying expression of purified TRP120-FL, -  
841 TR, -N, -C-terminus and TRX recombinant proteins. All listed recombinant proteins were  
842 expressed in a pBAD vector containing a His-tag.

843

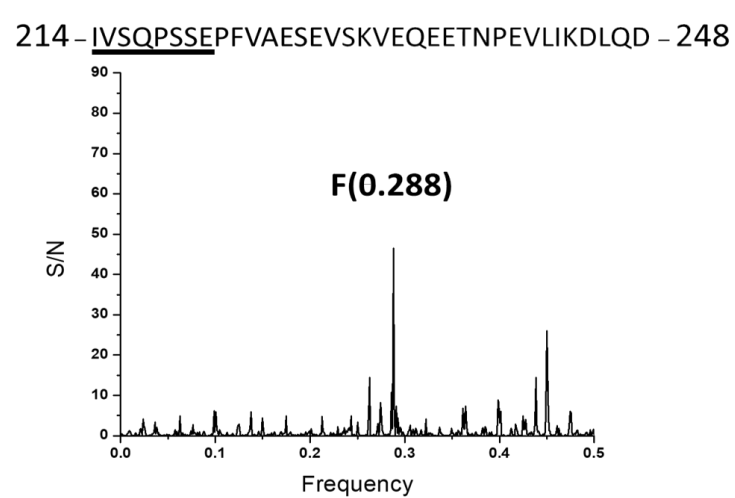
844 **Fig. S3. Jagged-1 activates Notch gene expression in a concentration-dependent manner.**  
845 Scatter plots of expression array analysis of 84 Notch signaling pathway genes to determine  
846 Notch gene expression with 1 ng/ml (top left). 10 ng/ml (top right) 100 ng/ml (bottom left) of

847 recombinant Jagged-1 at 24 p.t. Purple lines denote a 2-fold up or down regulation in  
848 comparison to control, and the black lines denotes no change.

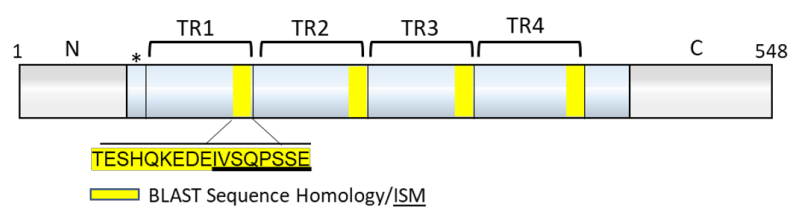
A.

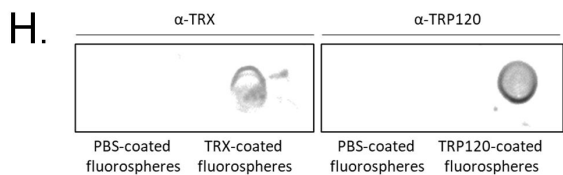
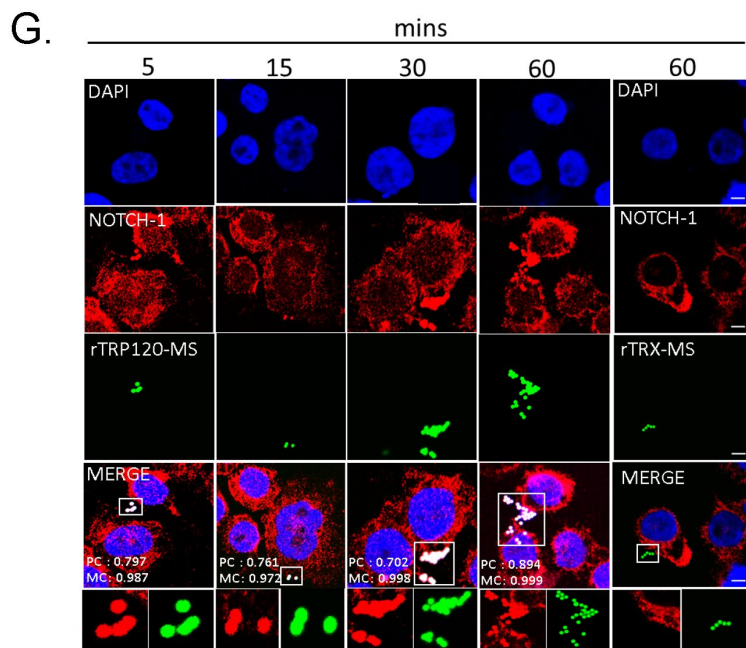
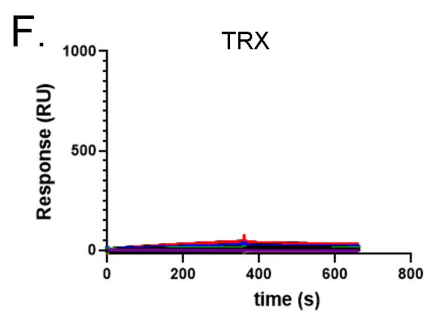
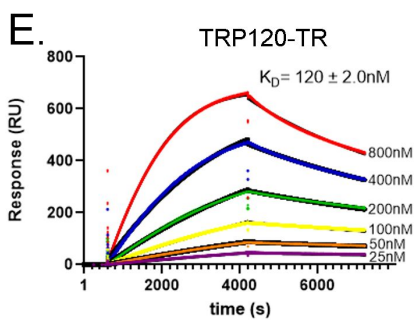
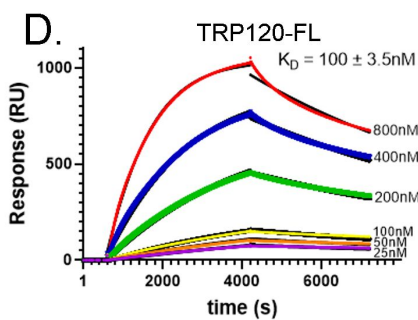
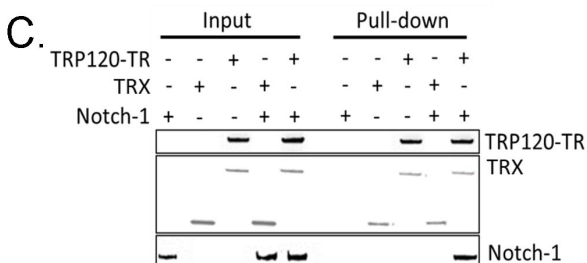
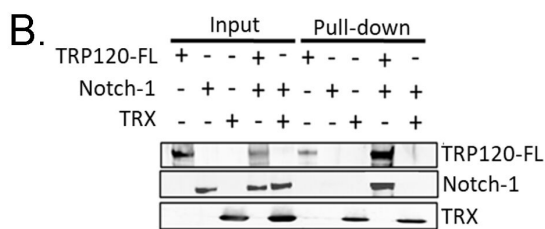
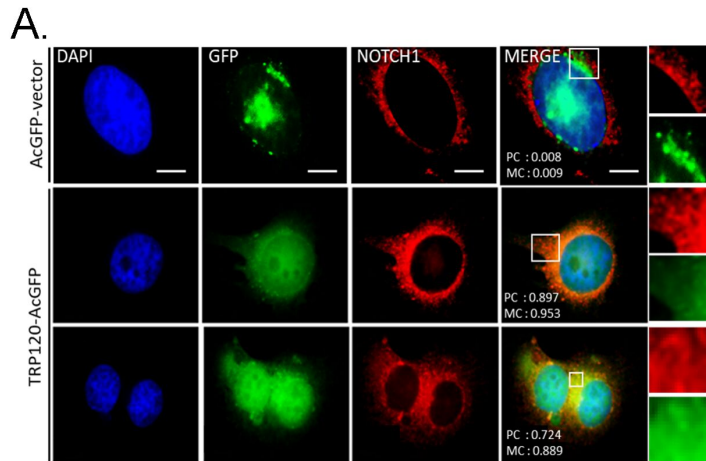
TRP120	284-TESHQKEDEIVSQPSSE-301
Jagged-1	1160-HNSEVEEDMDKHQQKA-1172
TRP120	284-TESHQKEDEIVSQPSSE-301
DLL1	655-RDAHSKRDTK-CQPQGS-671
TRP120	284-TESHQKEDEIVSQPSSE-301
DLL4	397-SNCEKKVDRCTSNPCAN-413
TRP120	284-TESHQKEDEIVSQPSSE-301
TSP2	970-VIRHQGK-ELVQTANS-999

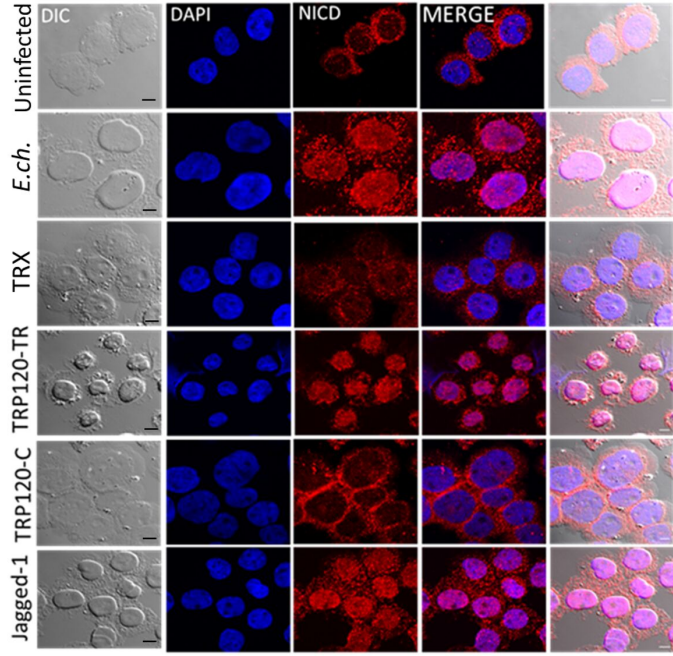
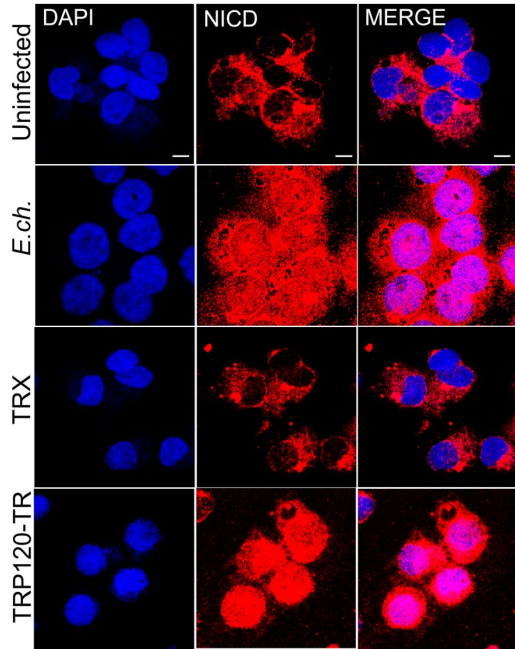
B.

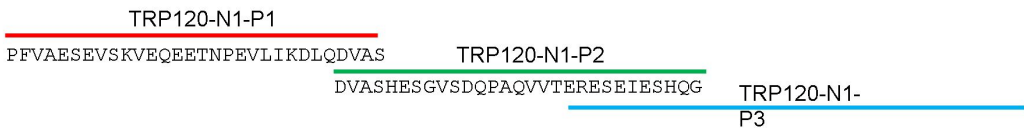
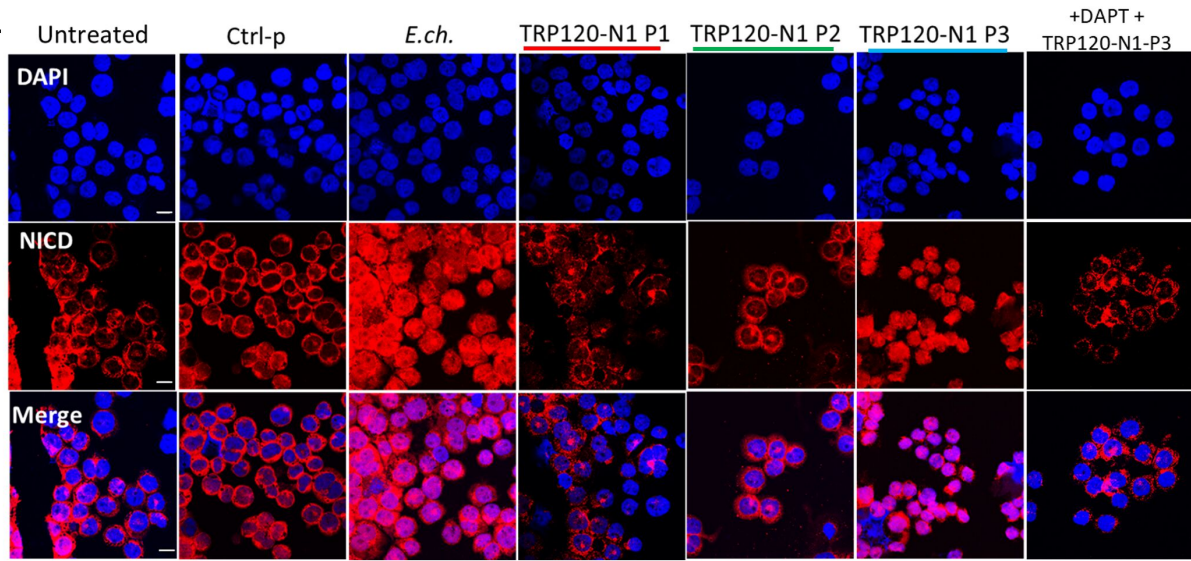
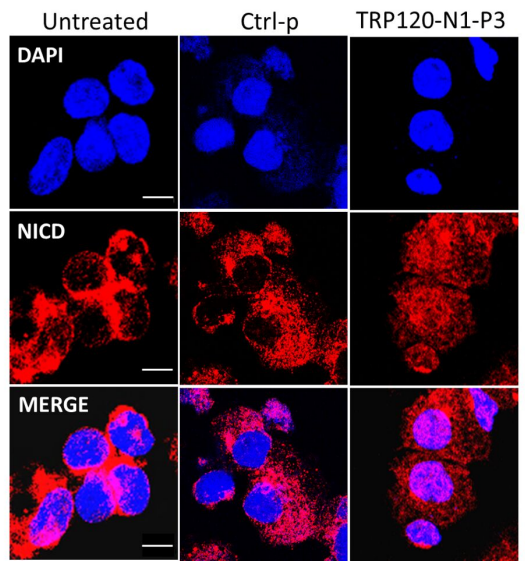


C.





**A.****B.**

**A.****B.****C.**



**A.**

Gene Symbol	Fold Regulation
CD44	9.77
DLL1	11.16
DLL3	10.14
DLL4	436.97
DTX1	538.76
HES1	86.35
HES5	43.98
HEY1	108.88
HEY2	205.31
HEYL	2.47
PAX5	1622.97
POFUT1	82.42
PPRAG	46.65
PSEN1	64.59
PTCRA	-1.94
SH2D1A	-7.67
ADAM17	9.84
JAG1	654.18
JAG2	90.37
MAML1	32.92
MAML2	34.17
NOTCH2	-2.43
NOTCH3	112.67
FZD4	18.40
GLI1	36.43
SUFU	126.99

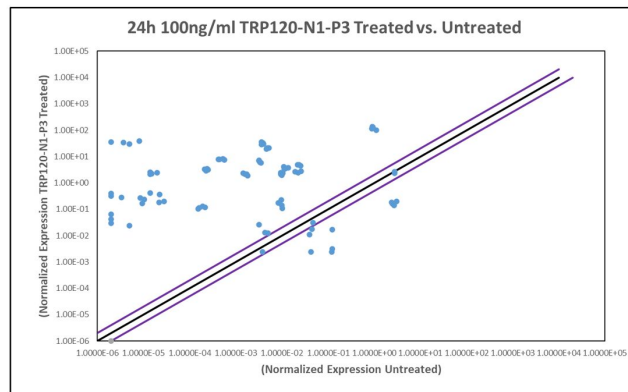
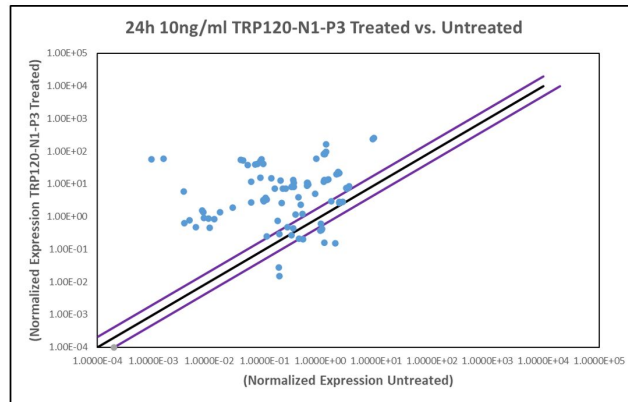
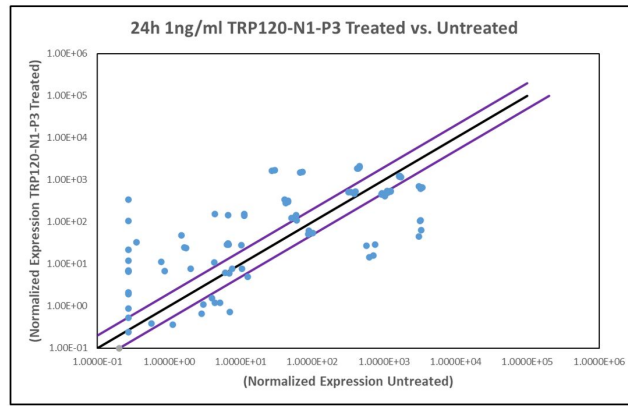
Notch target genes

Notch pathway components

Wnt and SHH pathway components

● Upregulated ● Downregulated ● Unchanged

**B.**

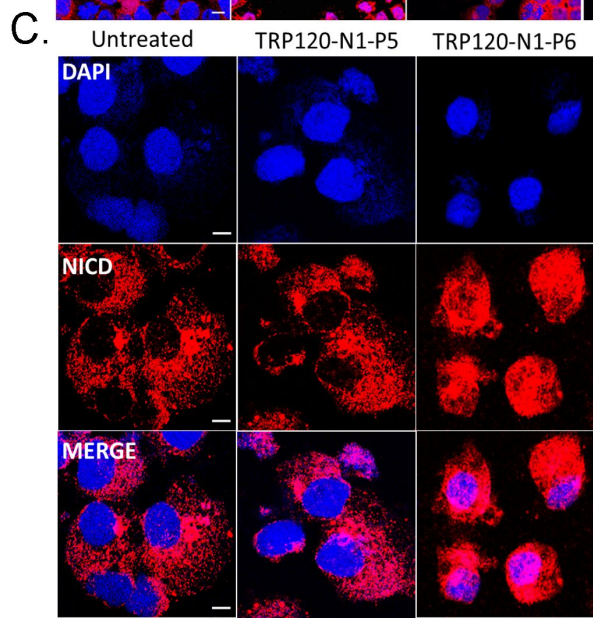
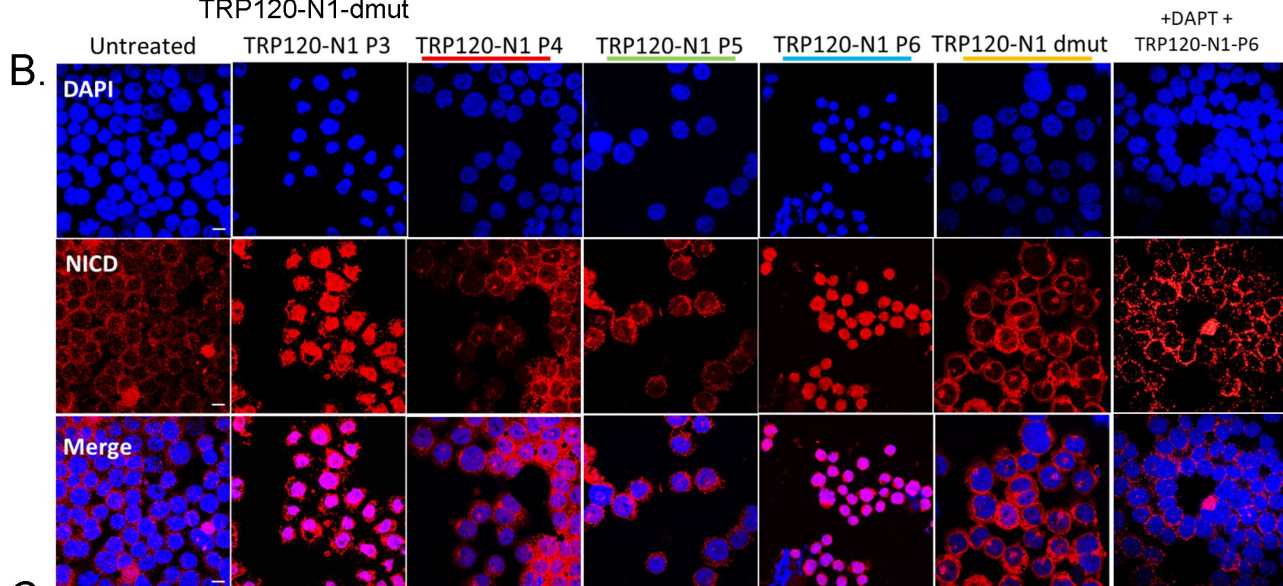


A. TRP120-N1-P3

RESEIESHQGETEKESGITESHQKEDEIVSQPSSE

TRP120-N1-P4    TRP120-N1-P5    TRP120-N1-P6

TRP120-N1-dmut



A.

Gene Symbol	Fold Regulation
CD44	20.74
DLL1	15.53
DLL3	12.75
DLL4	407.22
DTX1	477.81
HES1	25.77
HES5	220.74
HEY1	145.40
HEY2	193.21
HEYL	5.73
PAX5	349.38
POFUT1	177.47
PPRAG	192.04
PSEN1	52.40
PTCRA	1.37
SH2D1A	-8.36
ADAM17	14.29
JAG1	723.27
JAG2	46.73
MAML1	50.46
MAML2	92.38
NOTCH2	0.86
NOTCH3	223.35
FZD4	22.17
GLI1	39.78
SUFU	157.74

Notch target genes

Notch pathway components

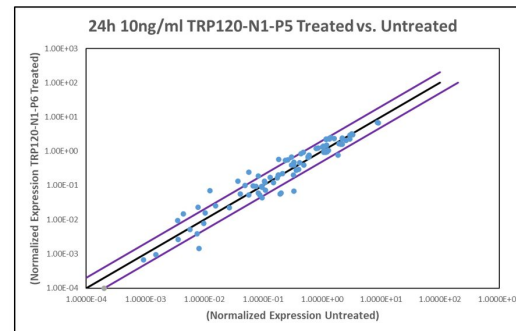
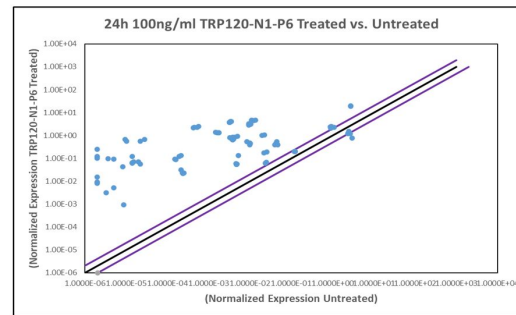
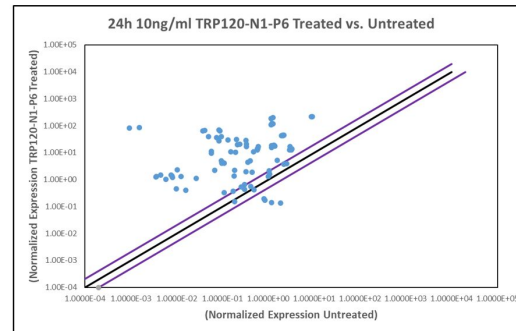
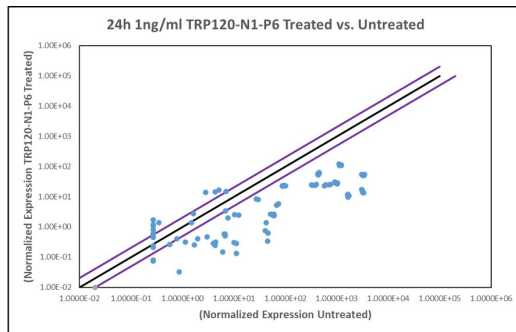
Wnt and SHH pathway components

● Upregulated

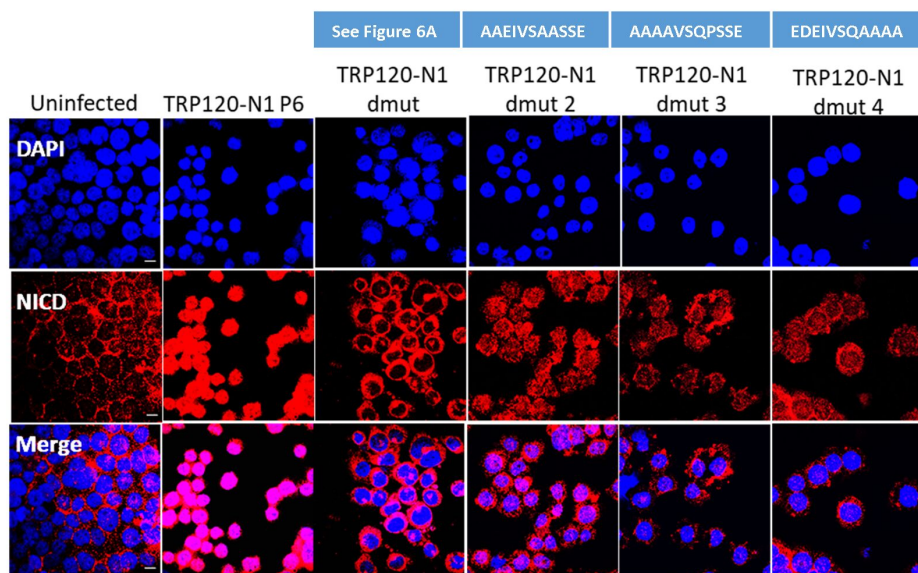
● Downregulated

● Unchanged

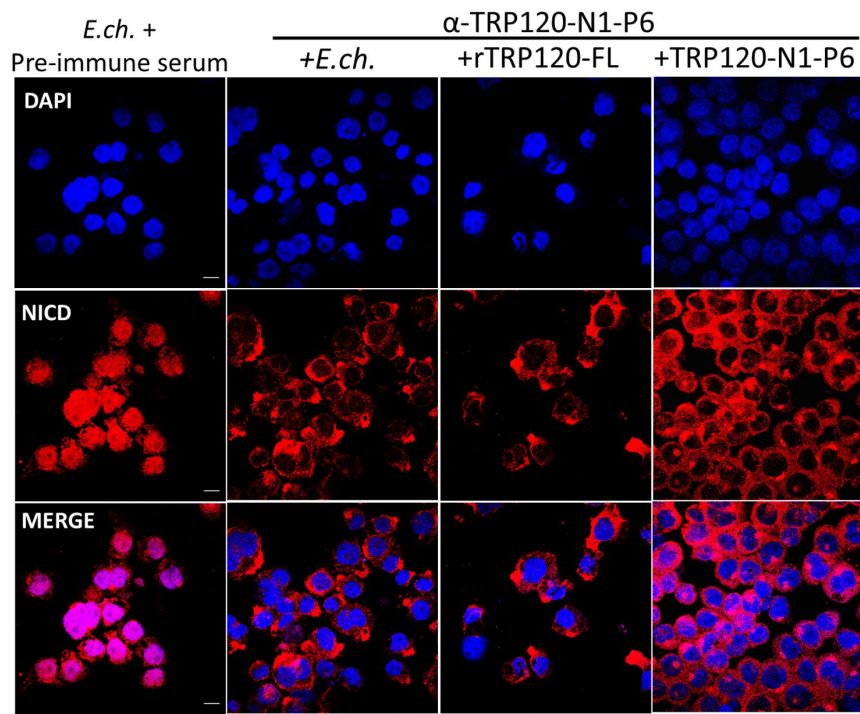
B.

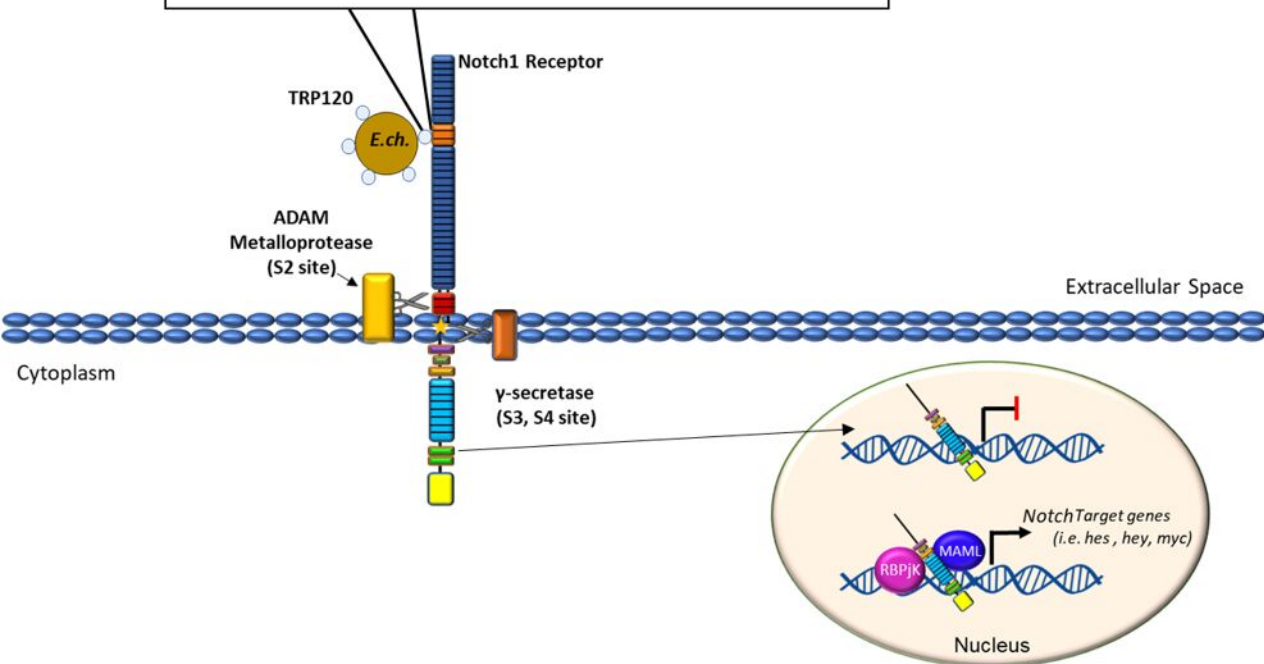
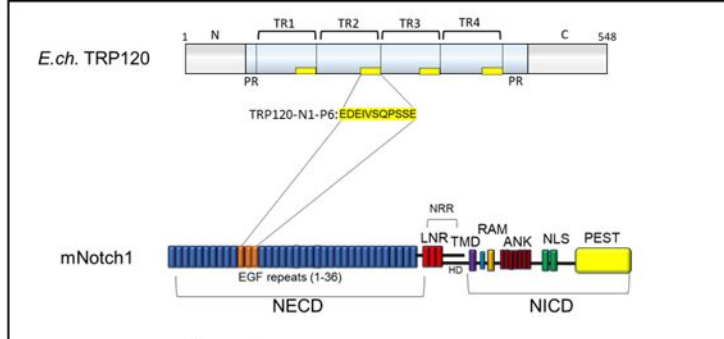


A.



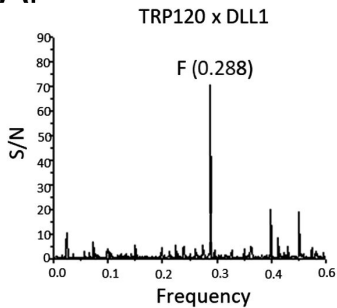
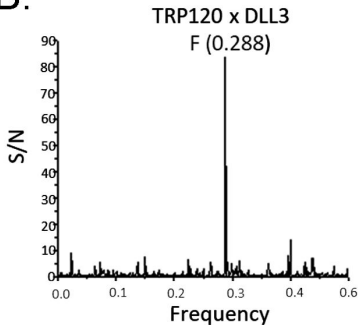
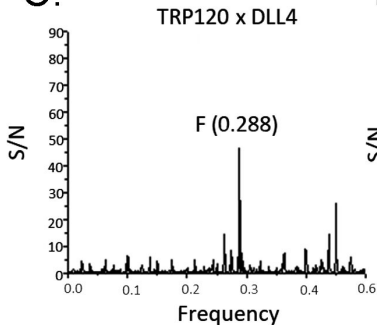
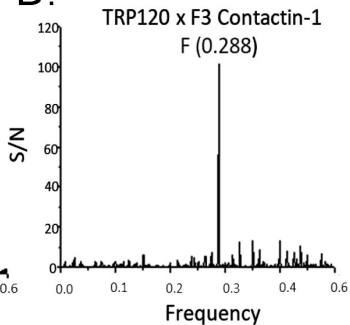
B.



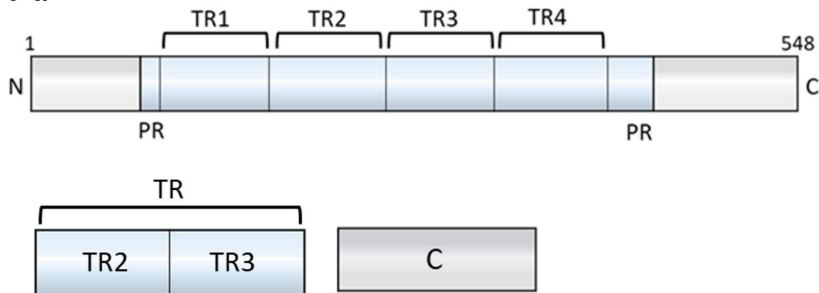


\*RBPjK: DNA-binding protein

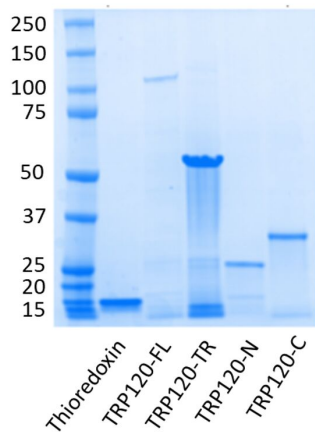
\*MAML: co-activator

**A.****B.****C.****D.**

A.



B.

**Expected Sizes:**

Thioredoxin: 16kDa

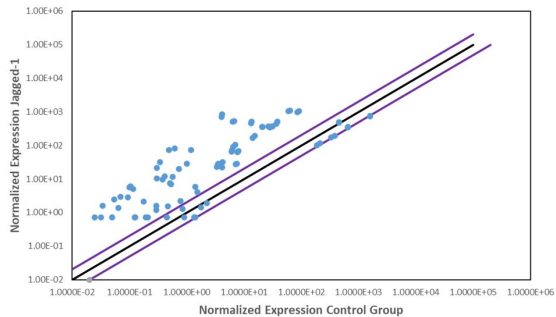
TRP120-FL: 120kDa

TRP120-TR: 52kDa

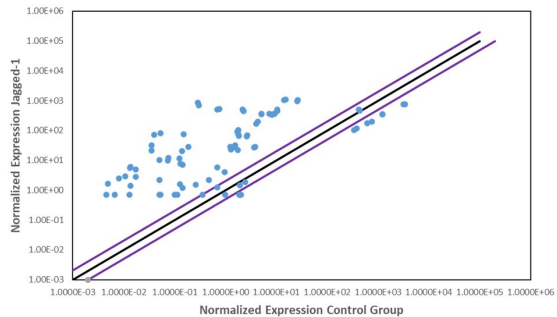
TRP120-N: 23kDa

TRP120-C: 32kDa

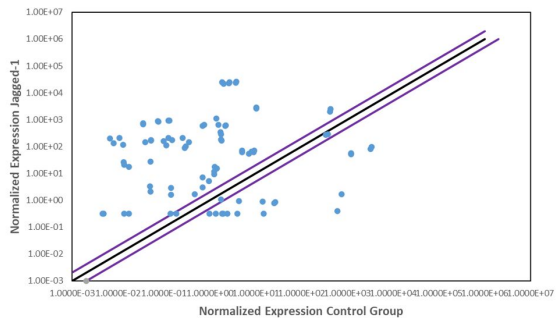
24h 1ng/ml Jagged-1 Treated vs. Untreated



24h 10ng/ml Jagged-1 Treated vs. Untreated



24h 100ng/ml Jagged-1 Treated vs. Untreated



1.0000E-03 1.0000E-02 1.0000E-01 1.0000E+00 1.0000E+01 1.0000E+02 1.0000E+03 1.0000E+04 1.0000E+05 1.0000E+06 1.0000E+07